REPORT NO. FR-79-73-538
HAC REF. NO. E2380

LEVEL II

ELECTRO-OPTICAL AND
DATA SYSTEMS GROUP
HUGHES
HUGHES AIRCRAFT COMPANY

HIGH ENERGY OPTICAL RESONANCE TRANSFER LASER STUDY

HUGHES AIRCRAFT COMPANY
CULVER CITY, CALIFORNIA 90230

JANUARY 1979

Mid-Term Technical Report for Period
24 July 1978 – 31 December 1978

SPONSORED BY
Defense Advanced Research Projects Agency
DARPA Order No. 2062, Amendment No. 19

MONITORED BY
Mr. Wayne Whitney, NRL Code 5540, under
Contract No. N00173-78-C-0470

CONTRACT EFFECTIVE DATE: 24 July 1978
CONTRACT EXPIRATION DATE: 24 July 1979

MISSING PAGE
NUMBERS ARE BLANK
AND WERE NOT
FILMED

SECURITY CLASSIFICATION OF THIS PAGE (When Data Entered)

REPORT DOCUMENTATION PAGE

READ INSTRUCTIONS BEFORE COMPLETING FORM

1. REPORT NUMBER

2. GOVT ACCESSION NO.

3. RECIPIENT'S CATALOG NUMBER

4. TITLE (and Subtitle)
High Energy Optical Resonance Transfer Laser Study.

5. TYPE OF REPORT & PERIOD COVERED
Mid-Term Technical Report.
24 July to 31 December 1978.

6. PERFORMING ORG. REPORT NUMBER
HAC-FR-79-73-538, HAC-REF-F238

7. AUTHOR(s)
P./Baily, J./Finzi, G./Holleman, K./Hui, and J./Wang

8. CONTRACT OR GRANT NUMBER(s)
N00173-78-C-0470

9. PERFORMING ORGANIZATION NAME AND ADDRESS
Hughes Aircraft Company
Centinela and Teale Streets
Culver City, CA 90230

10. PROGRAM ELEMENT, PROJECT, TASK AREA & WORK UNIT NUMBERS
DARPA Order No. 2062
Amendment No. 19

11. CONTROLLING OFFICE NAME AND ADDRESS
Defense Advanced Research Projects Agency
1400 Wilson Boulevard
Arlington, VA

12. REPORT DATE
January 1979

13. NUMBER OF PAGES
65

14. MONITORING AGENCY NAME & ADDRESS (if different from Controlling Office)
Naval Research Laboratory
4555 Overlook Ave., S.W.
Washington, D.C.

15. SECURITY CLASS. (of this report)
Unclassified

15a. DECLASSIFICATION/DOWNGRADING SCHEDULE

16. DISTRIBUTION STATEMENT (of this Report)
None

DISTRIBUTION STATEMENT A
Approved for public release
Distribution Unlimited

17. DISTRIBUTION STATEMENT (of the abstract entered in Block 20, if different from Report)
None

18. SUPPLEMENTARY NOTES
None

19. KEY WORDS (Continue on reverse side if necessary and identify by block number)
Optical Pumping,
HF Laser,
DF Laser,
HCN Laser,
Transfer Lasers

79 01 24 060

20. ABSTRACT (Continue on reverse side if necessary and identify by block number)
This report describes the first half of an experimental study of the HF laser pumped Optical Resonance Transfer Laser (ORTL). Several molecular systems were investigated including HF/HBr, HF/DF, HF/HCl, and HF/HCN as well as the optically pumped HF laser. The latter exhibited the best overall performance in quantitative fluorescence spectroscopy experiments and laser demonstration experiments. New laser systems demonstrated were optically pumped HF, and the HF/DF (3.8μ) and HF/HCN (3.9μ) ORTL systems. (Over)

micrometers

next page LB

DD FORM 1 JAN 73 1473 EDITION OF 1 NOV 65 IS OBSOLETE

409 084

SECURITY CLASSIFICATION OF THIS PAGE (When Data Entered)

Laser oscillation was achieved at pressures ranging from 25 torr to 110 torr. A maximum output power of 20 watts was achieved in the optically pumped HF laser.

SUMMARY

Quantitative fluorescence spectroscopy measurements and laser demonstration experiments were conducted with the objective of screening a number of potentially efficient HF laser pumped Optical Resonance Transfer Laser (ORTL) systems. The optically pumped HF laser and the HF/DF, HF/HBr, HF/HCl, and HF/HCN molecular systems were investigated. The best performance was achieved with the optically pumped HF laser, and the remainder of the program will concentrate on this system.

New laser systems successfully demonstrated were the optically pumped HF laser system, and the HF/DF and HF/HCN ORTL systems. Laser oscillation was observed at 41 Torr in all systems. The optically pumped HF laser was also demonstrated at pressures ranging from 25 to 110 Torr. Output spectra showed the power to be distributed among four to five lines in the $v = 2 \rightarrow v = 1$, and $v = 1 \rightarrow v = 0$ vibrational bands, with $P_2(8)$, the dominant output transition, sometimes containing as much as 78 percent of the output power. Powers up to 20 watts were outcoupled with the efficiency of conversion of absorbed pump radiation to laser radiation reaching 35 percent. Comparisons of the various molecular systems under similar conditions were made.

PREFACE

The work discussed in this report is possible because of prior work supported by Hughes Independent Research and Development funds, by the Ballistic Missile Defense Advanced Technology Center under Contract DASG60-77-C-0056, and by the Defense Advanced Research Projects Agency under Contract No. N00173-77-C-0174. The work is also influenced by a simultaneous effort dealing with DF pumped laser systems supported by Air Force Avionics Laboratory under Contract F33615-78-C-1477. This report was authored by P. K. Baily, J. Finzi, G. W. Holleman, K. Hui, and J. H. S. Wang. The authors would like to acknowledge the technical guidance provided by F. N. Mastrup. We would also like to acknowledge the assistance of H. Injeyan, C. Lovejoy, L. Marabella, R. Shimazu, and L. Williams in performing the experiments.

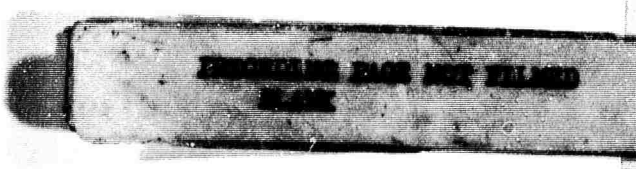

CONTENTS

ILLUSTRATIONS

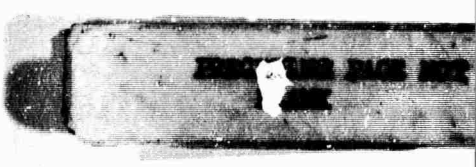

ILLUSTRATIONS (Continued)

TABLES

1.0 INTRODUCTION

1.1 BACKGROUND

High energy chemical lasers for DARPA applications should exhibit near diffraction limited beams in order to generate the required target irradiance levels at minimum size and weight. Because of problems associated with maintaining the chemical laser medium homogeneity, with the multiline nature of chemical lasers and with the complexity of the resonator design of the preferred cylindrical chemical laser configuration, it is difficult to achieve near diffraction limited beams directly. One promising approach to solving this problem is to use the high energy chemical laser as an optical pump for exciting a second single line output laser, applying the recently demonstrated Optical Resonance pumped Transfer Laser (ORTL)* technique. With this technology, the original stringent mode and medium requirements on the high energy chemical laser are significantly relaxed and the cylindrical chemical laser resonator arrangement decisively simplified. Because the role of the chemical laser is reduced to that of a source of primary optical power only, multi-mode characteristics of the chemical laser are no longer detrimental. The output beam control function of the total laser system is relegated in this new approach to a second laser, the ORTL. The two functions of the laser system, to generate power and to concentrate that power into a highly confined beam, can be physically separated. Of course, the premise that is fundamental to the ORTL approach to the high energy laser system problem is that each of these two functions can be solved separately in a more optimum way, so that better far field target irradiance can be achieved with the chemical laser ORTL system than by directly focusing the same primary chemical laser power onto the target.

The ORTL technique as originally demonstrated made use of two molecules, a donor and an acceptor, as the ORTL medium. The chemical laser (DF) served as the optical pump exciting the donor (DF) molecules in the ORTL cell. This donor then collisionally transferred its energy to an

---

*J. H. S. Wang, J. Finzi, and F. N. Mastrup, Appl. Phys Lett. 31, 35 (1977).

acceptor (CO_2) molecule which then became the active laser molecule for the ORTL. Subsequent to the original D^-/CO_2 (10.6 μ) demonstration, this technique was extended to DF/HBr (4.1 μ) and DF/N_2O (10.8 μ) systems.* In addition, a similar process in which only one molecule (DF) was present in the ORTL cell was demonstrated.** In this optically pumped DF laser system, the DF molecule served as both donor and acceptor. The DF molecules absorbed on the transition of the chemical pumping laser and excitation from one vibrational band to a higher band was achieved. Then, the energy was redistributed among the rotational levels of each vibrational band as the systems approached rotational equilibrium. As this occurred, population inversions on non-pumped vibration-rotational transitions were achieved and laser oscillation occurred. There was, of course, a slight wavelength shift.

The issues that must be addressed before either approach can become a practicable and preferred solution to the space laser beam control issue are whether very high conversion efficiency from multi-line HF or DF chemical laser power into single line ORTL power is achievable, and whether adequate medium homogeneity to permit the extraction of near diffraction limited beams at realistically scaled output power levels is possible. In order to gain the detailed technical understanding with which to address these issues, the present program was undertaken. Because the primary interest for DARPA applications is in HF lasers, it was decided that the program would concentrate on HF laser pumped systems. Prior work had dealt exclusively with DF laser pumped systems.

1.2 PROGRAM OBJECTIVES AND STRUCTURE

The primary objective of the present program is to develop a detailed understanding of the ORTL technique through well chosen laboratory experiments and analysis of the results. The program is oriented to be an experimental study, as opposed to a theoretical one. An associated goal of the

---

*Hughes IR&D, 1978

**4.3 Micrometer Laser Demonstration Experiment, Contract No. N00173-77-C-0174, Final Report, December, 1977.

program is to apply the attained understanding to the assessment of the potential of the technique for DARPA application through scaling analysis.

The program is structured into five tasks. The two major experimental tasks are a Screening Task and an ORTL Characterization Task. The major activity in the Screening Task was the performance of experimental measurements to screen a number of candidate systems with the objective of choosing one particular system for detailed study in the remainder of the program. This task was to be performed in the first three months of the program using existing apparatus. It was successfully completed on schedule. The systems screened in the laboratory were HF/HBr (4.1μ), HF/DF (3.8 μ), HF/HCN (3.1 and 3.9μ), and HF/HCl (3.8μ) as well as optically pumped HF (2.8 μ). The experimental results are presented in Section 2 which forms the bulk of this report. Following this task, the ORTL Characterization Task comprises a detailed experimental study of the chosen system. This task, concentrating on the optically pumped HF system, is in progress. Most activity to date, however, has been associated with analysis, experimental design, and new diagnostic apparatus construction. Consequently the space in this report devoted to this task is limited (see Section 3.1), consisting mainly of a brief description of the new measurements to be made. The results will be presented in the Final Report. In addition to these two tasks, there are two smaller experimental tasks: Chemical Laser/ORTL Dynamics Characterization and ORTL Output Beam Characterization. These are both scheduled for the second half of the program. Finally, there is a Scaling Analysis Task consisting of the use of Hughes' ORTL model and the experimental results of the other tasks to project the future capability of the ORTL technique. The technical approach to this task is discussed in Section 3.2.

1.3 SUMMARY OF RESULTS

The primary experiments utilized in the Screening Task were quantitative fluorescence spectroscopy of the ORTL medium and ORTL laser demonstration experiments. Both were combined with monitoring of the chemical pumping laser spectral distribution and power. The gas dynamic parameters (pressure, temperature, velocity, and composition) of the ORTL

medium were monitored in all experiments. Laser demonstrations involved both closed cavity and outcoupled ORTL resonators in which both laser power and spectral composition were monitored. In order to assure the generation of useful and measurable data in these experiments, the HF chemical pumping laser performance was first optimized for ORTL application. This optimization procedure involved power and spectral distribution measurements and the use of a computer model generated figure-of-merit which enabled the selection of the most effective chemical laser operating conditions.

A complete discussion of the Screening Task experiments is presented in Section 2, but the most significant technical accomplishments will be briefly previewed here. In the course of the Screening Task experiments, several new laser systems were demonstrated. They were the HF/DF (3.8 μ) and the HF/HCN (3.9 μ) ORTL systems, and the optically pumped HF (2.8 μ) system. The first two systems were demonstrated at 41 Torr, while the optically pumped HF system was operated over a range of pressures extending from 25 Torr to 110 Torr. The best performance was achieved with the latter system. Outcoupled power reached a high of 20 watts, and small signal gain in excess of 3 percent/cm was observed. Output spectra indicated that as much as 78 percent of the power was associated with a single vibration-rotational transition even though no attempt at line selection was made. A number of efficiency measurements were made and are presented in Section 2. Overall efficiency of conversion of incident pumping power to outcoupled ORTL power reached a high of 5.3 percent. Recognizing that no effort has been made at optimizing the geometry to achieve high absorption of the pumping radiation, it would appear that the efficiency of conversion of absorbed power to ORTL optical power is more indicative of eventual performance limitations. The maximum achieved value for this quantity was 34.5 percent. In assessing the significance of these results, it should be remembered that the effort to date was a process of screening various candidates. Consequently no significant effort at performance optimization was made. In fact, calculations indicate that much higher efficiencies can ultimately be achieved. (Significantly higher efficiencies should be

demonstrated in the second half of this program.) Based upon the relative performance of the systems investigated, it was decided upon completion of the Screening Task that the major emphasis in the remainder of the program would be on the optically pumped HF laser system.

2.0 SCREENING TASK

2.1 OBJECTIVE

The objective of the Screening Task was to obtain experimental data which would allow a meaningful comparison of the various molecular systems under consideration. The most important result of this task would then be a recommendation of a single system for intensive investigation in the Characterization Experiments of Task 2. The short time alotted to this task and the consequent limitation to available apparatus placed certain restrictions on the variety of measurements which could be made and on the number of molecular systems which could be investigated. Furthermore, each molecular system could not be investigated in detail. However, a performance comparison under common conditions could be made.

These considerations made it imperative to quickly identify a group of systems for investigation and an appropriate methodology for achieving the objective of this task. Prior to this contract, experimental work at Hughes had included only the DF laser pumped systems. These included the optically pumped DF laser as well as the DF/CO_2, DF/HBr, and DF/N_2O ORTL systems. Because the primary interest for DARPA applications is in HF chemical lasers, it was decided to concentrate on HF laser pumped systems. This data could then be evaluated and compared to prior data on DF pumped systems. The molecular systems chosen for study on this program were optically pumped HF, and the following ORTL systems: HF/DF, HF/HBr, HF/HCN, and HF/HCl. All were investigated during the Screening Task.

2.2 TECHNICAL APPROACH

The approach to this task consisted of a well-defined sequence of experiments, each designed to guide the next set of experiments. After an initial period of diagnostic improvements during which the ORTL cell gas flow, fluorescence spectroscopy, and pumping laser performance measurements were all improved, a series of experiments were performed on the HF chemical laser to be used as the optical pump in screening experiments. These chemical laser experiments, described in detail below, were designed to optimize optical pump performance. Chemical laser output power, beam

dimension and quality, and laser radiation spectrum were monitored under a variety of operating conditions. This data was then evaluated with the aid of Hughes' ORTL model to assess relative pumping efficiency under a defined set of ORTL operating conditions. Effective chemical laser operating conditions were then chosen for use in the ensuing fluorescence experiments. These fluorescence experiments monitored via quantitative fluorescence spectroscopy the excited vibrational-rotational state population densities in the ORTL cell HF molecules as well as in the various acceptor molecules. Data from this set of experiments were then used to assess the probability of achieving a successful laser demonstration. Based upon these results, a series of laser demonstration experiments were defined and executed. Several of the optically pumped systems exhibited lasing action, while others could not be made to lase under the available laboratory conditions. Each successful lasing demonstration described below represents the first demonstration of that particular system. The specific experiments and results which led to the choice of optically pumped HF as the recommended system are described in this Section.

2.3 MODEL DESCRIPTION

The previously developed Hughes ORTL computer model was used to guide and evaluate experiments in the Screening Task. The model describes a donor molecule, which is optically pumped, and an acceptor molecule. For each of these molecules five vibrational levels including the ground state are considered. With inputs of different molecular constants, the donor-acceptor pairs of HF/DF, HF/HCl, HF/HBr, and HF/HCN have been modelled. The optically pumped HF system is constructed by decreasing the concentration of the acceptor to a negligible amount. In this model, the principal processes consist of:

1. Resonance optical pumping of the donor molecules
2. V-V exchange collisions among donor molecules
3. V-V exchange collisions among acceptor molecules
4. V-V transfer collisions between donor and acceptor molecules
5. V-T quenching processes of donor and acceptor molecules.

It is assumed that both donor and acceptor are always in rotational equilibrium. This assumption may not be appropriate at all pressures especially when lasing occurs. The kinetic rate data for the kinetic processes are obtained from the literature.* These data include deactivation rates of molecules in v = 1 and higher levels and temperature dependences of these rates.

Based on the kinetic and pumping processes, rate equations are written and differential equations for the population density in each vibrational level of the donor and acceptor molecules are derived. These differential equations are solved numerically in the computer code using a subroutine which employs the Adam-Moulton method with the predictor-corrector step control. The temperature of the gas medium affects the pumping and kinetic processes and is evaluated in each step of integration from the total heat released in the quenching, V-V exchange, and transfer processes using a constant pressure assumption. As a function of position along the ORTL flow direction (or interaction time), the population densities and small signal gains for donor and acceptor levels are calculated. In the lasing case when the small signal gain is larger than the threshold level (determined by total cavity losses), the gain is fixed at this level and excess population appears as photons. At the time of the Screening Task, lasing was permitted only on a $v = 1 \rightarrow v = 0$ or $v = 2 \rightarrow v = 1$ transition and only on one rotational line in the band.

In using the model to evaluate the experimental results, experimental conditions are used as input parameters to the code. These include the observed optical pumping flux in each vibration-rotational pumping line, the

*References:

Handbook of Chemical Lasers, R. W. F. Gross and J. F. Bott ed., J. Wiley & Sons, N. Y., 1976.

N. Cohen, "A Review of Rate Coeff ents in the H_2-F_2 Chemical Laser Systems - Supplement (1977), "SAMSO-TR-78-41, The Aerospace Corp., CA, 1978.

M. A. Kwok and R. L. Wilkins, J. of Chem. Phy. 63, 2453 (1975).

M. A. Kwok, Private Communication.

initial gas temperature, the gas composition, the flow velocity, and the interaction geometry. The output parameters which include the number density for each vibration level in the donor and the acceptor, the gas temperature as a function of interaction time, the outcoupled power, and the absorbed power can then be used to predict experimental results.

2.4 PUMPING LASER OPTIMIZATION

When there is a short absorption path in the ORTL cell, the chemical laser optical pump must be carefully matched to the ORTL conditions in order to optimally transfer power from the pump laser beam to the ORTL gas. Important parameters that need to be considered are pumping flux W, pump spectral distribution, and pump absorption efficiency η_i. The optical pumping rate constants are directly proportional to W; the spectral distribution of the pump beam sets limits on the population distributions that can be achieved; and the absorption efficiency is an important factor in determining the overall efficiency of a particular ORTL configuration. In the Screening Task the pumping flux and spectral distribution were of prime importance, because the configuration was fixed and the absorption efficiency could only be changed by changing these two parameters. Variations in pumping configuration will be an important factor in the rest of the program.

It can be shown* that the limiting (i.e. infinite pumping flux) population ratio, $C_{v\infty}$, of the population in the v + 1 vibrational level to that in the v level of an optically pumped species, HF for example, where rotational Boltzmann equilibrium is maintained is given by

$$C_{v\infty} = \frac{[HF\ (v+1)]}{[HF(v)]} = \frac{B_{v+1} \sum_J J \exp\left[\frac{-hc}{kT} B_v J\,(J+1)\right]}{B_v \sum_J J \exp\left[\frac{-hc}{kT} B_{v+1} J\,(J-1)\right]} \qquad (1)$$

*Optical Resonance Transfer Laser Investigation, Contract No. DASG-77-C-0056, Final Report, February, 1978.

where P-branch ($\Delta J = -1$) radiation is used for pumping. In this expression B_v is the rotational constant of the v^{th} vibrational level, and J the rotational quantum number. With P-branch pumping $C_{v\infty}$ is always less than one, so only partial inversions are possible. Numerical evaluation of $C_{v\infty}$ shows that $C_{v\infty}$ is maximized at low J so the goal of the HF chemical laser optimization was to operate the chemical laser under conditions that emphasized low J lasing.

The HF laser was characterized for the purpose of optimizing ORTL performance by running a series of experiments with a constant reactant flow-rate into the combustor of 300 mmole/sec. The variable parameters were the diluent mole fraction in the combustor, β_{He}, the excess fluorine in the combustor, $\beta_{\Delta F_2}$ and the distance from the nozzle exit plane to the laser optic axis, X_c. The goal of the tests was to experimentally define the operating parameters that would result in very low J-level lasing with a minimum loss of total power. High diluent tends to increase low J-level lasing by reducing the temperature in the gain zone, but excessive diluent reduces the efficiency of fluorine atom production in the combustor. The presence of molecular fluorine in the laser cavity increases the temperature via the $F_2 + H$ "hot" reaction. Small amounts of excess fluorine can be dissociated more easily than large quantities so $\beta_{\Delta F_2}$ was the second parameter that was varied during laser characterization tests. Finally X_c was scanned because the chemical laser cavity temperature is a function of the downstream distance from the nozzle. The output powers and the smallest lower lasing level rotational J values obtained are shown in Figure 1 as a function of β_{He} for several of the experimental conditions. Typical outputs had approximately equal intensities in the $v = 1$ to $v = 0$ and $v = 2$ to $v = 1$ bands and negligible intensity in the $v = 3$ to $v = 2$ band. The maximum power output was approximately 1 kW with lower level J values of 6, 7, 8 and 9 for the $\beta_{\Delta F_2} = 0.10$ series and 700 W with lower level J values of 5, 6, 7 and 8 for the $\beta_{\Delta F_2} = 0.07$ series. Further reduction of $\beta_{\Delta F_2}$ to approximately 0.04 produced lasing to the $J = 4$ level.

Optimization of a chemical laser to obtain low J spectral output tends to reduce the total pump flux available. Thus it was necessary to develop a means to evaluate simultaneously the effect of variations in both

power and J-distribution. The relation between the two depends on the dynamics of the optically pumped ORTL populations so that optimum conditions can only be determined by using the ORTL model. ORTL gain is optimum when C_v is maximized, so model calculations of C_v were chosen as the figure of merit. In practice it is necessary to look at a single band, so that C_o was chosen. A standard ORTL system was selected, and ORTL performance was calculated as a function of the flux and J-distribution that was obtained in the laser characterization tests.

Figure 1 shows the variation in total pump flux that was observed when laser operating conditions were adjusted to optimize the J-distribution. For each of these laser pump conditions calculations were performed to predict the C_o value when the optically pumped system had reached "quasi-equilibrium". For example, the results in Figure 2 indicate that C_o has reached an approximately constant value after about 10 μsec of interaction. The subsequent slow increase in the C_o value is due to the increase in temperature of the gas medium. The value at a particular temperature in this "quasi-equilibrium" region may be used as a figure of merit. The C_o value

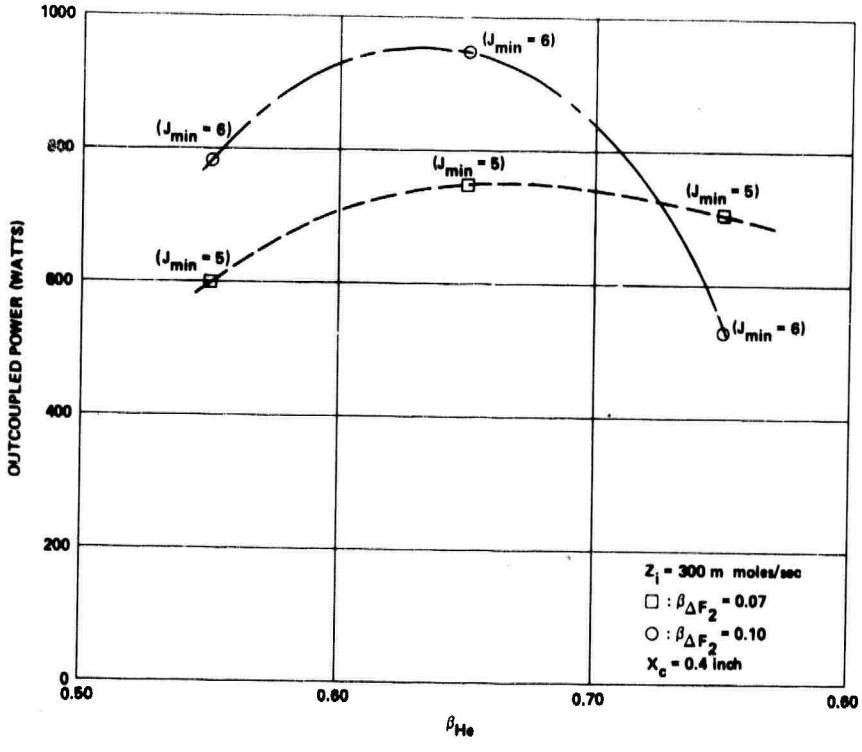

Figure 1. Results from the HF laser characterization experiments

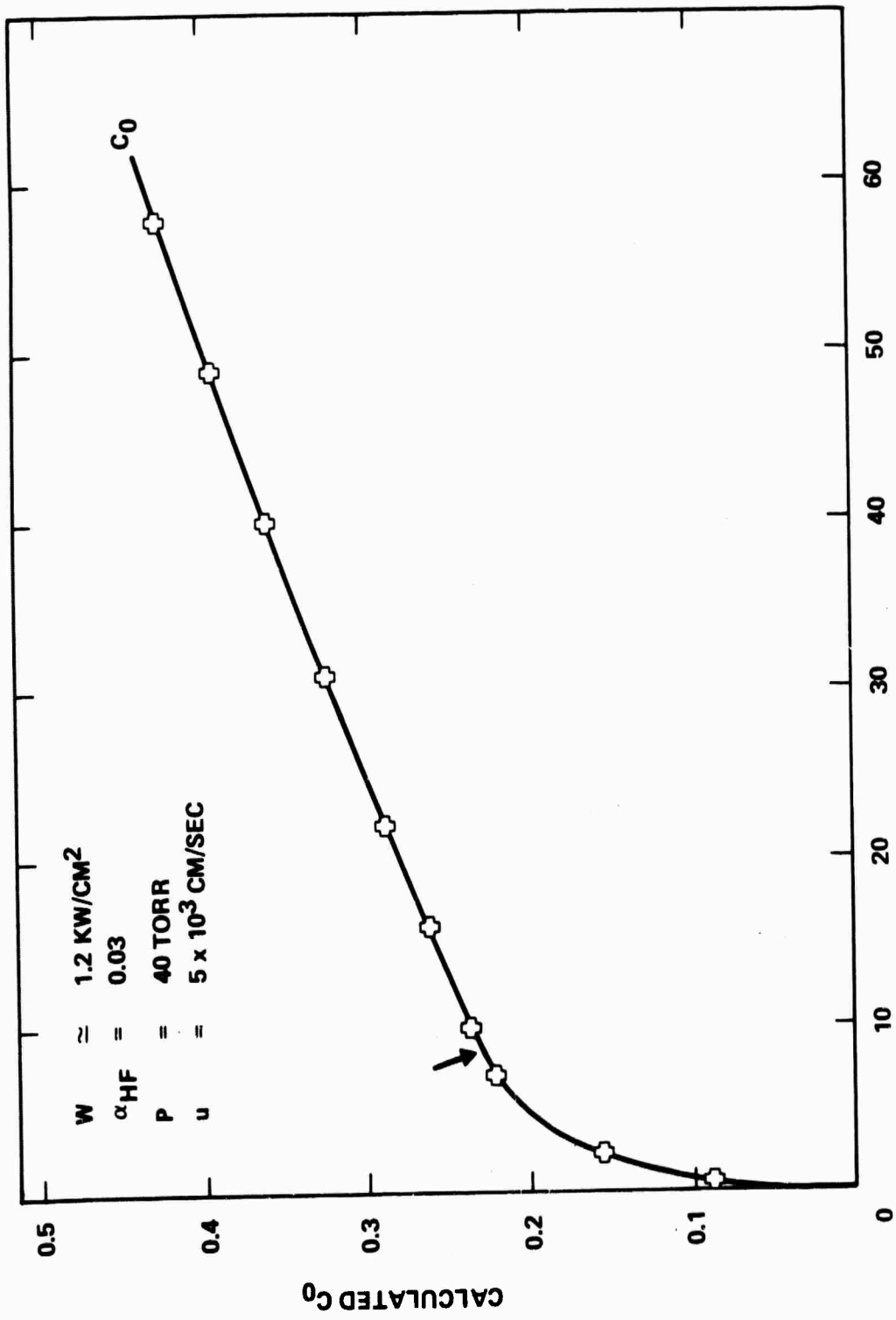

Figure 2. Calculated C_0 as a function of interaction time for optically pumped HF

at 330°K was selected for these particular conditions. Figure 3 shows the figures of merit calculated for the pump laser conditions of Figure 1, and a particular $\beta_{\Delta F_2}$ = 0.042 experiment. Clearly J-distribution is very important because the lower power condition produces the better figure of merit. The $\beta_{\Delta F_2}$ = 0.04 and 0.07 conditions were selected for use in the screening experiments.

The validity of these figure of merit calculations was subsequently verified for the optically pumped HF system in ORTL lasing experiments.

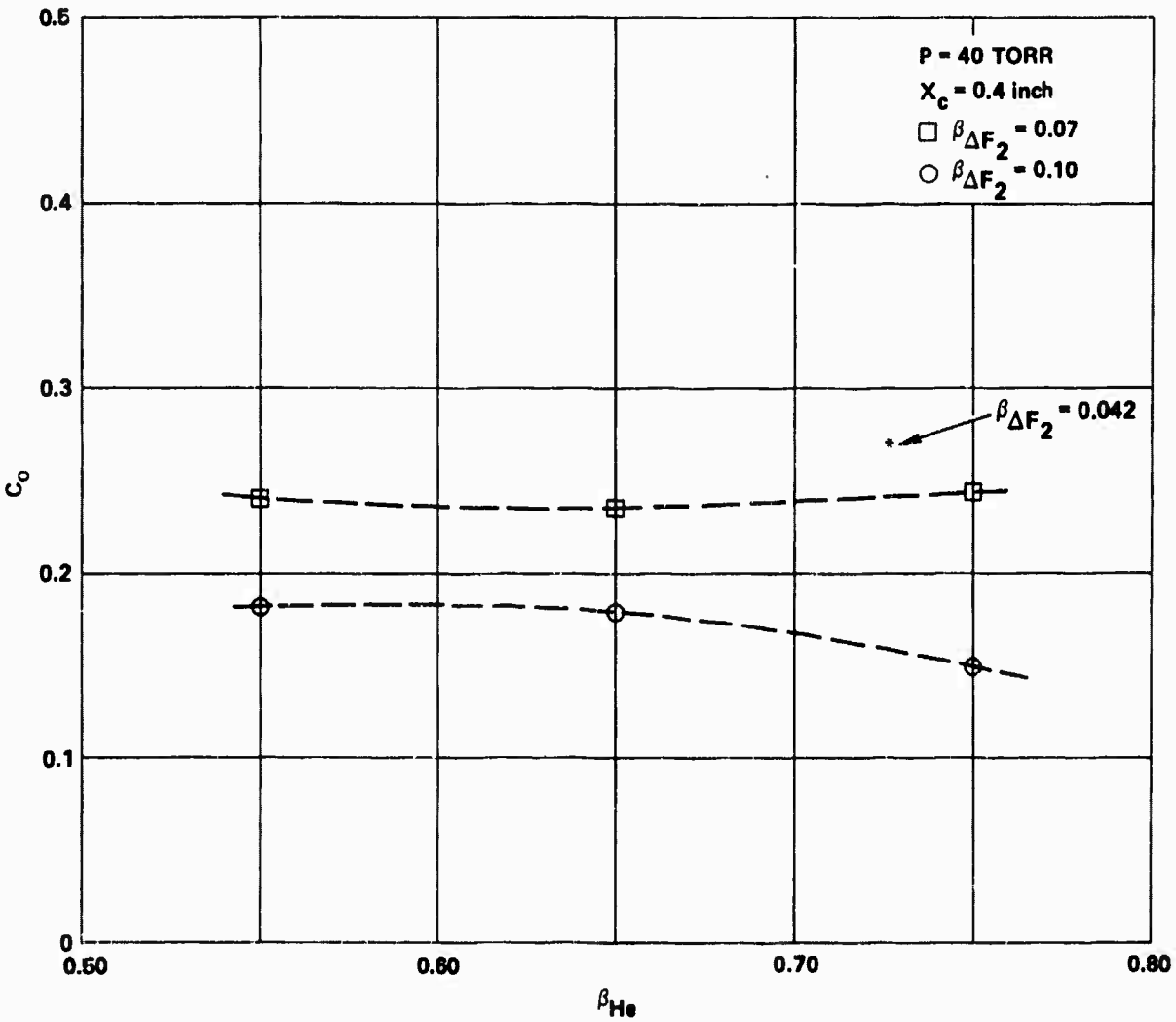

Figure 3. Figure of merit for the HF pumping laser

Figure 4 compares the ORTL power obtained with two pump laser conditions. The condition which yielded the $P_1(4)$ lasing line produced better ORTL performance under all ORTL conditions than the alternative where lasing started at $P_1(5)$ even though the flux was 50 percent higher in the latter case.

2.5 ORTL APPARATUS DESCRIPTION

A schematic of the apparatus used to conduct the Screening Task is shown in Figure 5. The apparatus was designed to allow continuous monitoring of the following: chemical laser total power and vibration-rotation spectrum, donor and acceptor fluorescence spectra, ORTL laser total output power and spectrum, as well as the pressure, temperature, and molar flow of all ORTL species. The apparatus description will be di ·ided into three parts: the chemical laser, the ORTL cell, and the diagnostics for fluorescence and lasing tests.

Chemical Laser

The operating principles of the combustion driven HF laser are well documented in the literature.* For use in the Screening Task experiments, an optical resonator was constructed with a three meter radius and a flat mirror spaced approximately 70 cm apart. The curved mirror was a water cooled metal substrate coated for maximum reflectivity at 2.8 μ. The flat out-coupling mirror was silicon and coated for 25 percent transmission at the same wavelength. The CaF_2 window which formed the vacuum seal for the laser, also split off 8 percent of the beam directing it toward power meter P_1 (Coherent Radiation Model 213). The remainder was focussed by either a cylindrical or spherical CaF_2 lens into the ORTL cell. An identical power meter at position P_2 was used for calibration of P_1 just prior to each experiment. Scattering from a secondary CaF_2 plate was collected and imaged onto a spectrometer (McPhearson 218) for recording the vibration-rotation line spectrum from the chemical laser. In this manner both the laser power and spectrum were continuously monitored throughout each run.

*Handbook of Chemical Lasers, R. W. F. Gross, ed., Wiley Interscience, 1976.

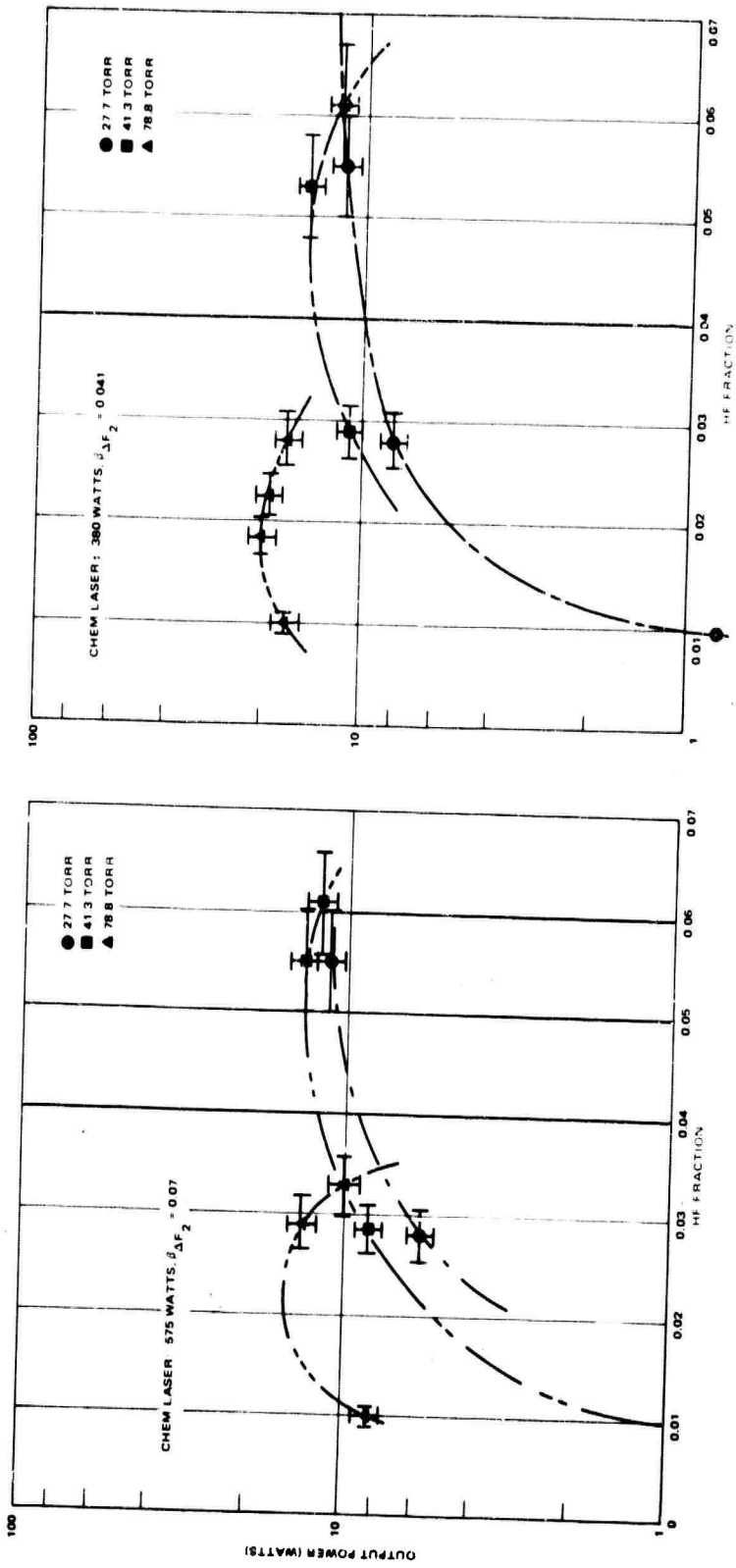

Figure 4. Optically pumped HF laser output power

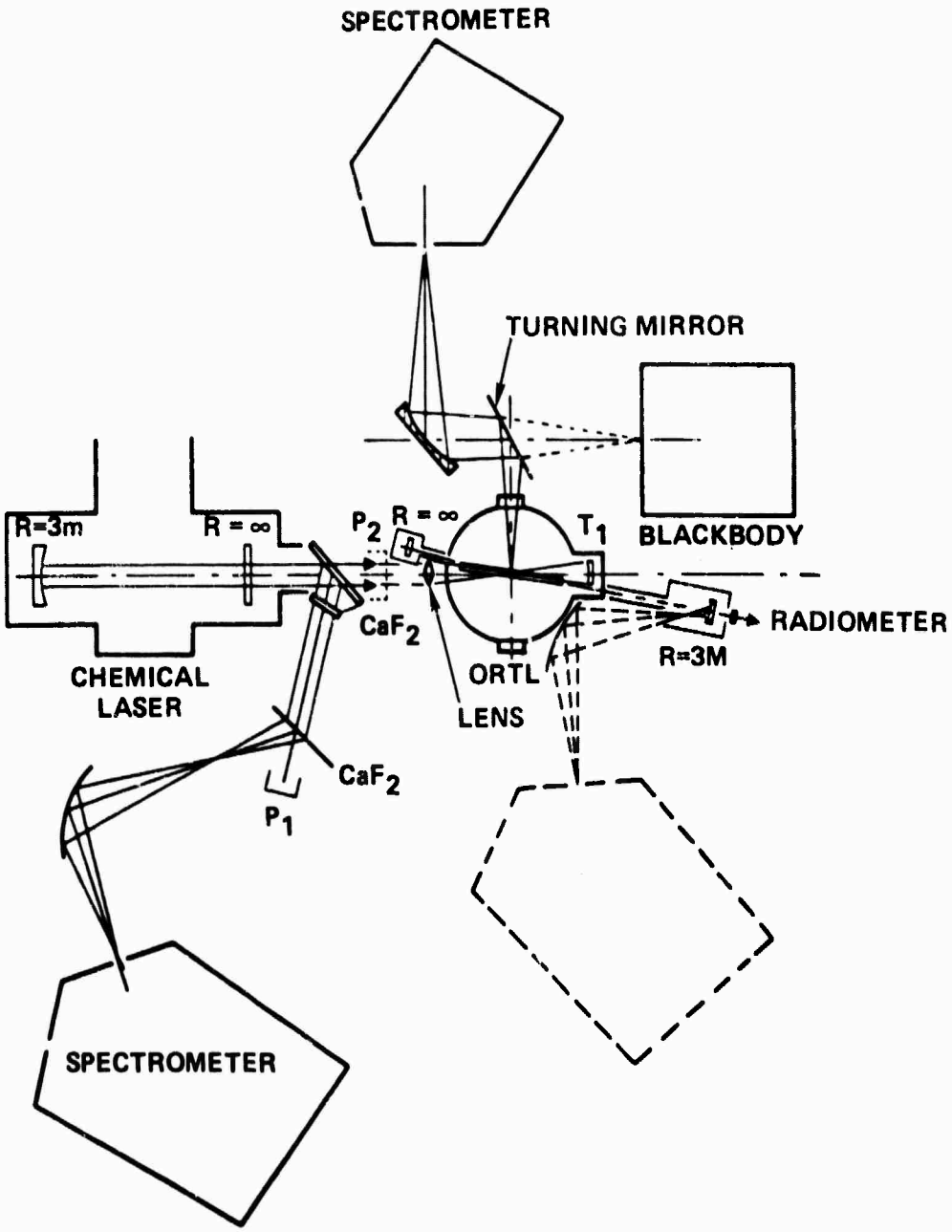

Figure 5. Apparatus configuration for screening task experiments

From the chemical laser optimization two standard chemical laser operating conditions were chosen, as discussed above. The first with a $\beta\Delta F_2$ of 0.067 gave 575 watts measured at the ORTL cell. The beam cross section when focussed with a cylindrical lens was 2.3 cm long by 0.38 cm high, resulting in an irradiance of 660 W/cm^2 at the ORTL cell center. With a spherical lens, the focussed beam dimensions were 8mm x 4mm producing 3 kW/cm^2 at the ORTL cell. With a $\beta_{\Delta F_2}$ of 0.042, 380 watts of pump power were produced yielding irradiances of 440 W/cm^2 and 2 kW/cm^2 for cylindrical and spherical focussing respectively. The power was distributed approximately equally between the lowest two vibrational bands for both conditions, as described earlier.

ORTL Cell

The ORTL cell used for fluorescence and lasing tests is shown in Figure 6a. Modular in construction, it contains a subsonic nozzle for the ORTL gas flow and a surrounding nozzle for a curtain gas flow which confines the ORTL gas as it flows through the lasing region. The ORTL nozzle is rotated with respect to the pump beam so that the effective gain length is longer than the length of the incoming beam. The ORTL nozzle can be rotated to allow 1.5, 2, or 3 times the length of the HF laser radiation. This rotation simultaneously increases the HF absorption path length by the same factor, as shown in Figure 6b. The ORTL cell includes ports for measuring the pressure and temperature of the ORTL flow stream. Thermocouples located downstream of the interaction zone are available to measure the temperature rise of the gas to estimate the power absorbed from the pump beam. A mirror placed at the opposite end of the cell refocusses the pump beam back onto the nozzle, doubling the pump flux. The long tubes projecting from the ORTL cell in Figure 6a, permit evacuable mirror boxes to be attached. Thus, a very low loss optical cavity devoid of Brewster windows is achieved. This feature is essential when attempting to lase low gain systems.

The required small flow rates of HF, and the various acceptor gases were regulated by a calibrated mass flow controller (Matheson 8249). Flow rates ranged between 0.1 and 2 mmoles/sec. The larger helium curtain and duct flows were controlled by calibrated sonic orifice meters. The gas mixture entering the ORTL cell was at ambient temperature for all experiments.

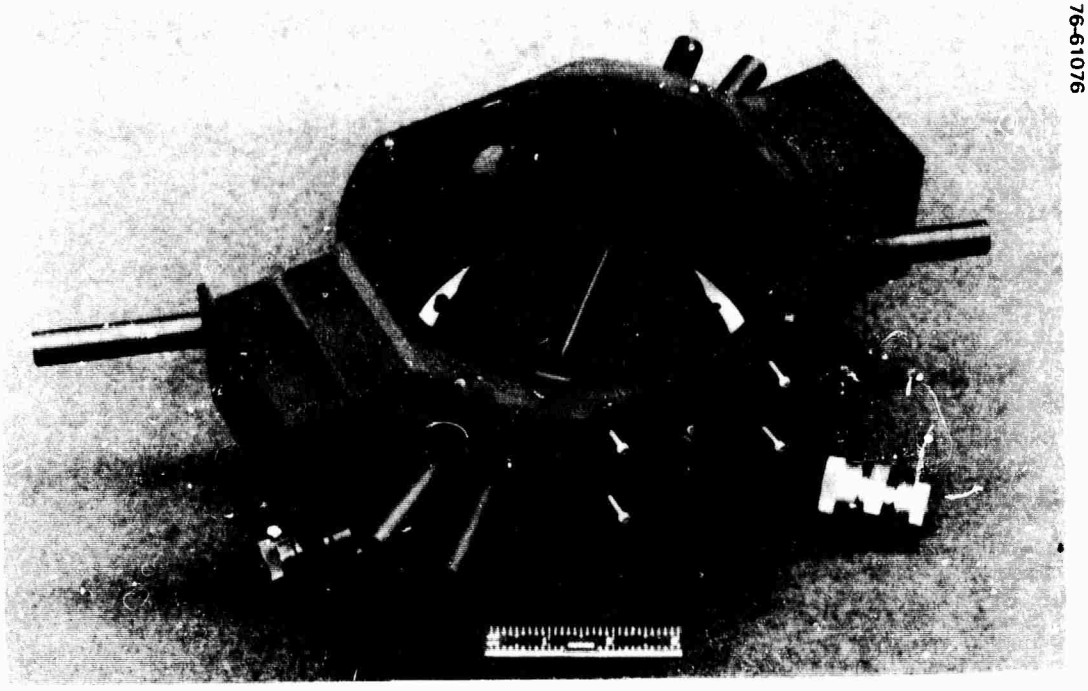

76-61076

Figure 6a. Rotated ORTL cell

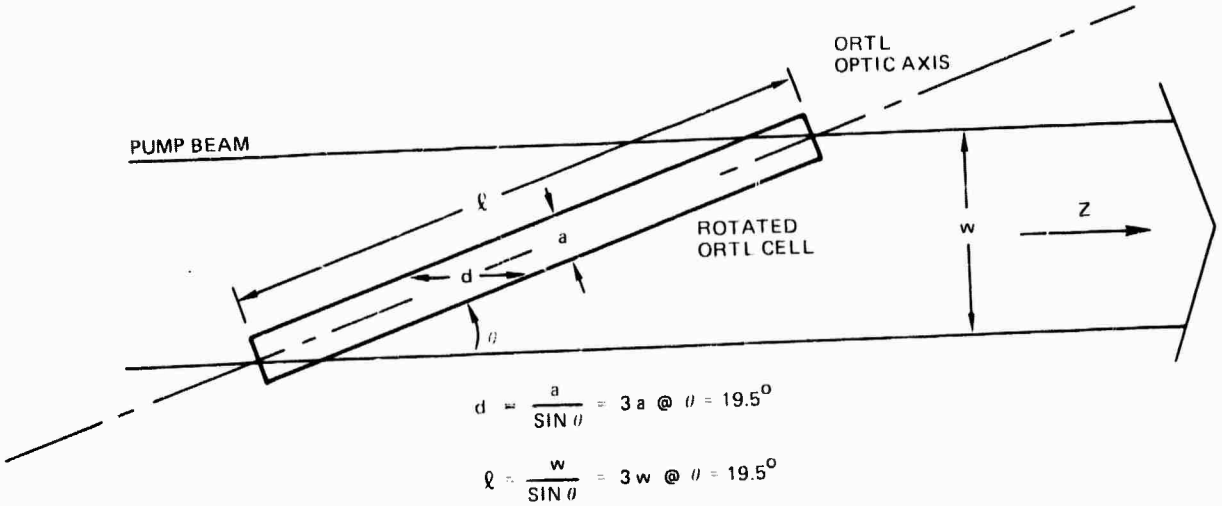

Figure 6b. Absorption length and gain length relations in rotated ORTL cell

Performance Diagnostics

The ORTL cell was equipped with two spectroscopy ports oriented at 90 degrees to the pumping direction. Emission from the ORTL gas molecules was imaged by a toroidal mirror onto the entrance slit of the scanning spectrometer (McPhearson 218). Phase sensitive detection utilizing an In:Sb detector and lock-in amplifier (PAR 124) permitted detection of weak fluorescence signals. Absolute infrared intensities were measured by illuminating the detector system optics with a blackbody (Electro-Optical Industries WS 155). This calibration was done "in situ" beforeand after each series of tests by removing the kinematically mounted turning mirror shown in Figure 5.

For laser demonstration experiments, the key parameters measured were output power and laser line distribution. The latter was measured with a scanning spectrometer similar to that already described above. The imaging geometry shown by dotted lines in Figure 5 had the toroidal imaging mirror defocussed to cover the surface of one of the resonator mirrors. Scattering from the resonator mirror allowed detection under closed cavity conditions where no ORTL optical power was outcoupled. Outcoupled power was obtained using a partially transmissive dielectric mirror, and measured with a pyroelectric radiometer (Laser Precision 3440) outside the mirror box. An added feature of this geometry was that it in no way interfered with the fluorescence apparatus, allowing simultaneous fluorescence and lasing spectra to be obtained.

2.6 FLUORESCENCE EXPERIMENTS

Infrared fluorescence measurements were undertaken for two reasons: to identify potential candidates for Screening Task laser demonstration experiments through quantitative measurements of excited state densities, and to obtain a data base with which to assess a system's overall potential. In addition, fluorescence measurements provide key data with which to gauge the accuracy of the computer model described earlier.

The HF/acceptor vibrational population distributions and the gas temperature at the excitation region are determined from analysis of the vibration-rotation fluorescence spectrum. The line emission intensity, I, originating

from the upper level with quantum numbers v'j' integrated along the optical path, l, is given by

$$I_{v'j'} = \frac{16\pi^3 \nu_o^4 c\, 10^{-7}}{3} \cdot S_{j'} \cdot |\mu|^2 \frac{\int N_{v'j'} dl}{2j' + 1} \text{ watts/cm}^2\text{-st} \qquad (2)$$

where ν_o is the wavenumber (cm^{-1}), c the speed of light, $S_{j'}$ the rotational line strength factor, μ the dipole transition moment, and $N_{v'j'}$ the number density of the v'j' state. The corresponding signal from the spectrometer is

$$S = I_{v'j'} \cdot \Omega \cdot A \cdot T_\lambda \cdot \alpha_\lambda \text{ volts} \qquad (3)$$

where S is the signal in volts, Ω the solid angle subtended by the collection system, A the spectrometer slit area, T_λ the transmission factor of all the optical components, and α_λ the detector responsivity at wavelength λ. When the same spectrometer system is calibrated against a blackbody the signal S_{BB} is,

$$S_{BB} = N_{BB} \cdot \Delta_\lambda \cdot \Omega \cdot A \cdot T_\lambda \cdot \alpha_\lambda \text{ volts} \qquad (4)$$

where N_{BB} is the spectral radiance of the blackbody and Δ_λ is the resolution of the spectrometer in centimeters. Substituting the Boltzmann factor for $N_{v'j'}$ in Equation (2), and combining Equations (2) through (4) yields

$$\frac{\int N_{v'j'} dl}{2j' + 1} = \frac{e^{-B_{v'} j'(j'+1)\frac{hc}{kT}}}{kT/hcB_{v'}} \int N_{v'} dl = \frac{N_{BB} \cdot \Delta_\lambda \cdot S}{[16\pi^3 \times 10^{-7} \nu_o^4 c\, S_{j'} |\mu|^2/3] \cdot S_{BB}} \qquad (5)$$

Inspection of Equation (5) shows that a plot of $\ln [\int N_{v'j'} dl/(2j'+1)]$ vs $j'(j'+1)$ should be linear if self absorption and rotational nonequilibrium effects are negligible. The negative slope of this line equals $hcB_{v'}/kT$, and the ordinate intercept equals $\ln [(hcB_{v'}/kT) \int N_{v'} dl]$. The temperature, therefore, can be

determined from the slope and the concentration from the intercept if path length is assumed to equal the dimensions of the nozzle. An example of such a plot is shown in Figure 7.

The ground state population cannot be determined spectroscopically. It is obtained from the difference of the total number density and the sum of all excited states, with appropriate corrections due to temperature rise and concomitant optical path increase. Consequently, the accuracy of this method falls short of a direct optical measurement. We estimate the latter to be ±15 percent and the former ±25 percent in these experiments.

The system studied most extensively was the optically pumped HF system. A representative HF emission spectrum is shown in Figure 8. A series of experiments were conducted in which the pressure was varied from 25 torr to 110 torr, and the HF mole fraction from 1 percent to 6 percent

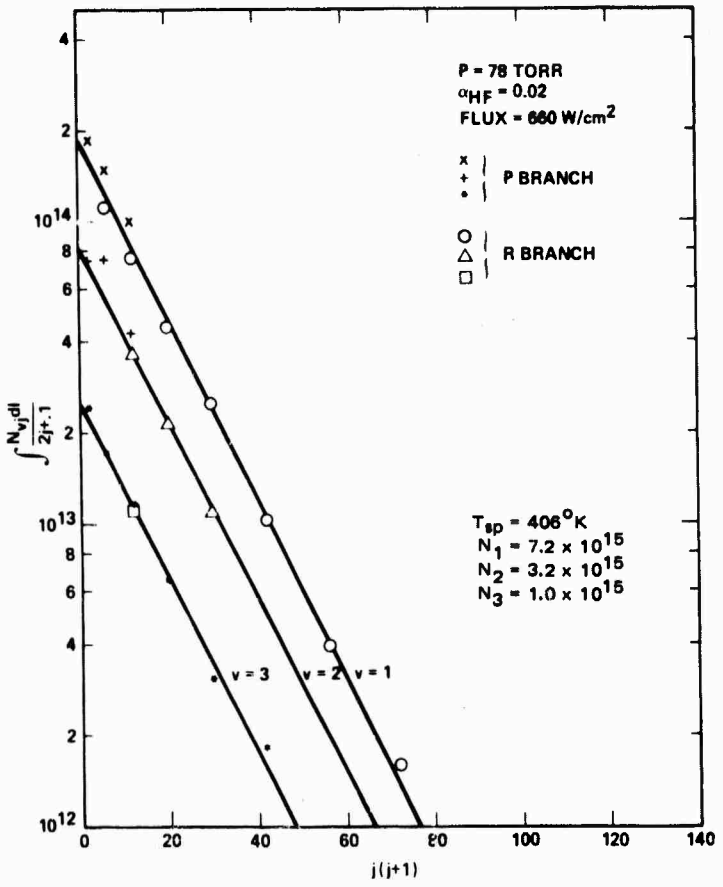

Figure 7. HF fluorescence spectrum analysis

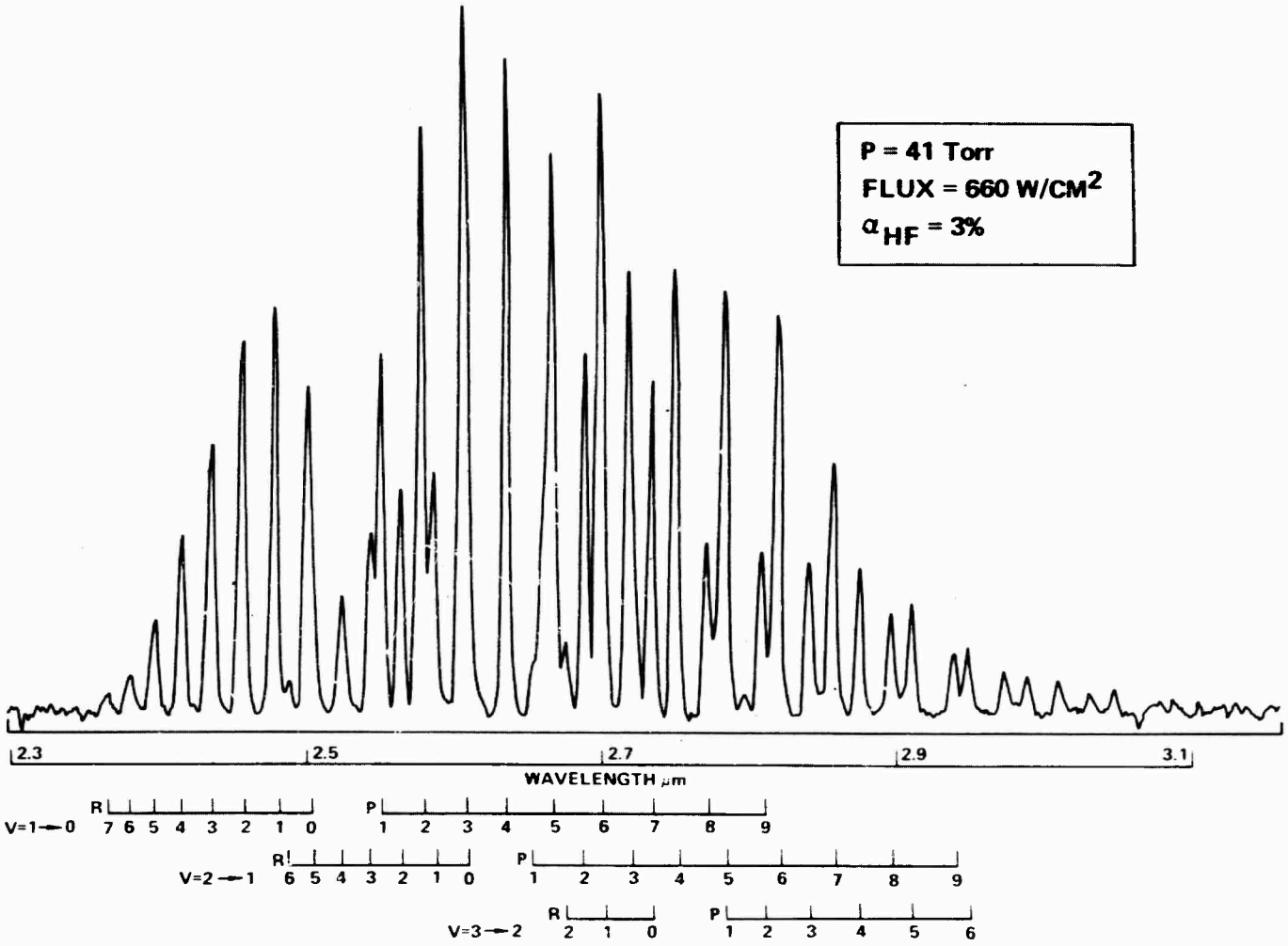

Figure 8. Optically pumped HF emission spectrum

with helium comprising the remainder of the gas. The velocity was kept fixed at 5×10^3 cm/sec. The irradiation geometry was deliberately chosen to be the same as anticipated for lasing experiments; the irradiance at the ORTL cell was 660 W/cm^2. The fluorescence optical length with a 3 mm wide x 6 cm long nozzle was 3.2 mm. (Refer to Figures 5 and 6 of the previous section.) The short path was essential to minimize self trapping of HF radiation.

The variation of excited state vibrational population with HF mole fraction is shown in Figures 9 to 11 for 25, 41, and 78 torr total pressure. The shaded curves are computer model predictions reflecting the uncertainties in the literature. The behavior of the spectroscopic temperature, corresponding to the gas temperature in the excitation zone, is shown in Figure 12 for the series at 41 torr. The bands represent variation of the HF V – T kinetic rate from the smallest literature value* of 1.6×10^{-12} cm^3/molecule-sec at 300°K to the largest value** of 2.7×10^{-12} cm^3/molecule-sec at 300°K. Considering the absence in the model of multiple quantum transitions and rotational nonequilibrium, the experimental and calculated results are in good agreement. The HF v = 1 and v = 2 populations are controlled by the optical radiation field. Higher HF vibrational states are populated by V-V collisions and are sensitive to the V dependence of the exchange and quenching kinetics. Assuming a $V^{2.3}$ dependence for HF V-T quenching and a harmonic oscillator dependence for V-V exchange gives the best match to experimental results.

The ratio of upper to lower level population is directly proportional to the small signal gain, with the threshold partial inversion ratios for diatomics typically ranging from 0.2 to 0.5. Figure 13 shows the variations of C_0, C_1 and C_2 with HF mole fraction at the three pressures investigated. From the relative magnitudes, HF (2 → 1) transitions would be expected to provide the strongest laser intensities.

---

*M. A. Kwok and R. L. Wilkins, J. Chem. Phys. 63, 2453 (1975).

**R.A. Luct and T.A. Cool, J. Chem. Phys. 60, 2554 (1974).

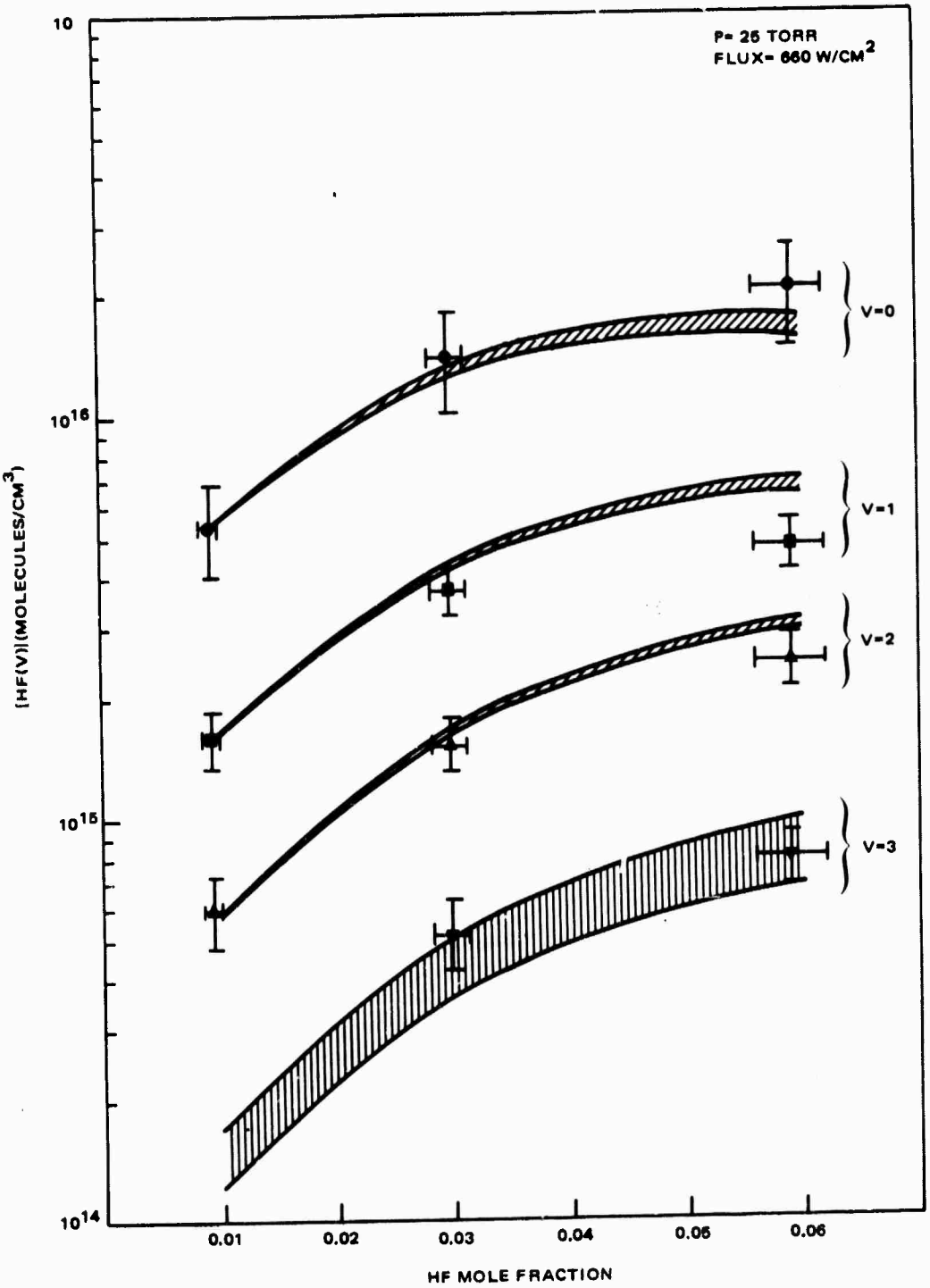

Figure 9. Optically pumped HF vibrational population densities (25 torr)

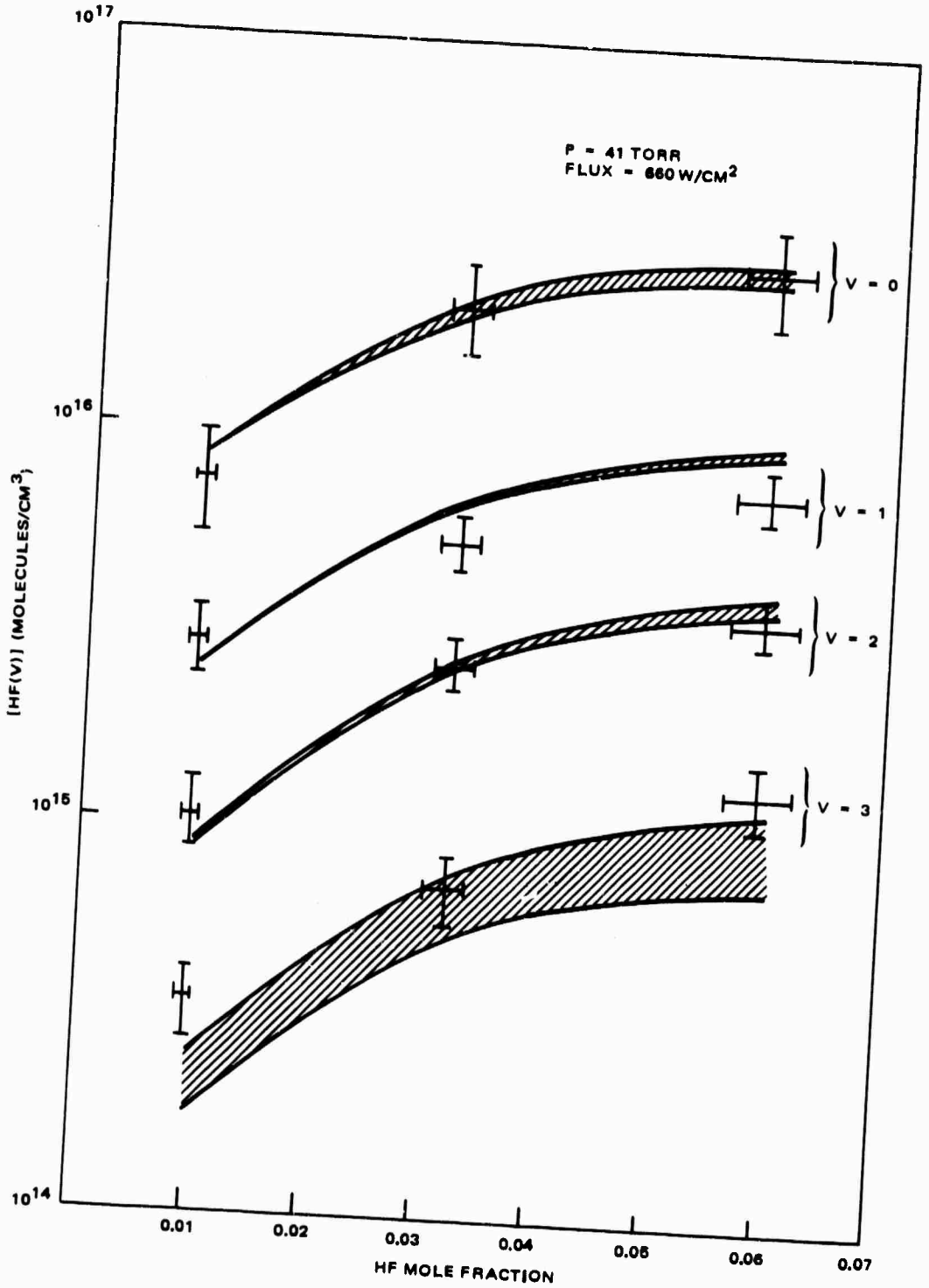

Figure 10. Optically pumped HF vibrational population densities (41 torr)

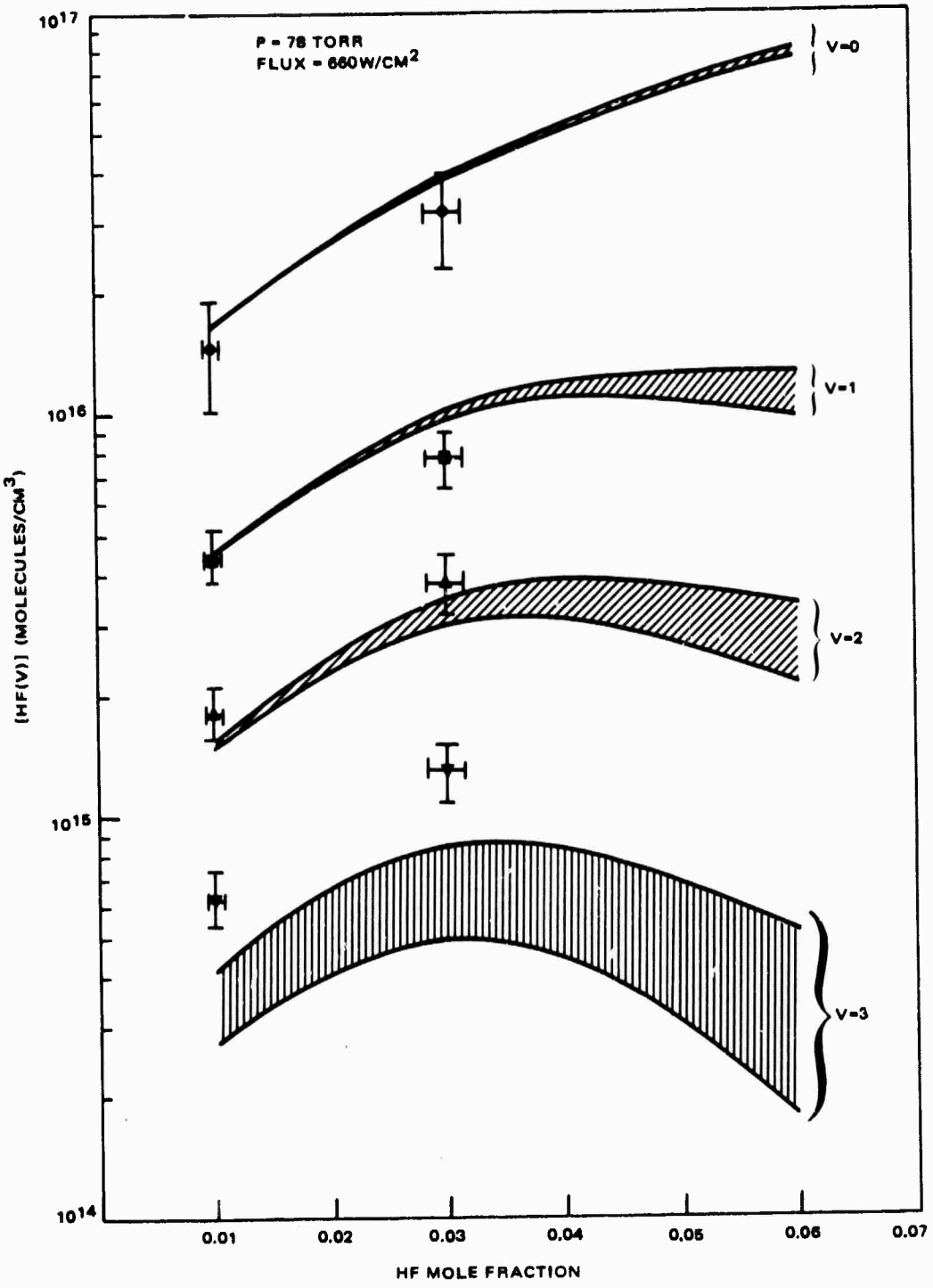

Figure 11. Optically pumped HF vibrational population densities (78 torr)

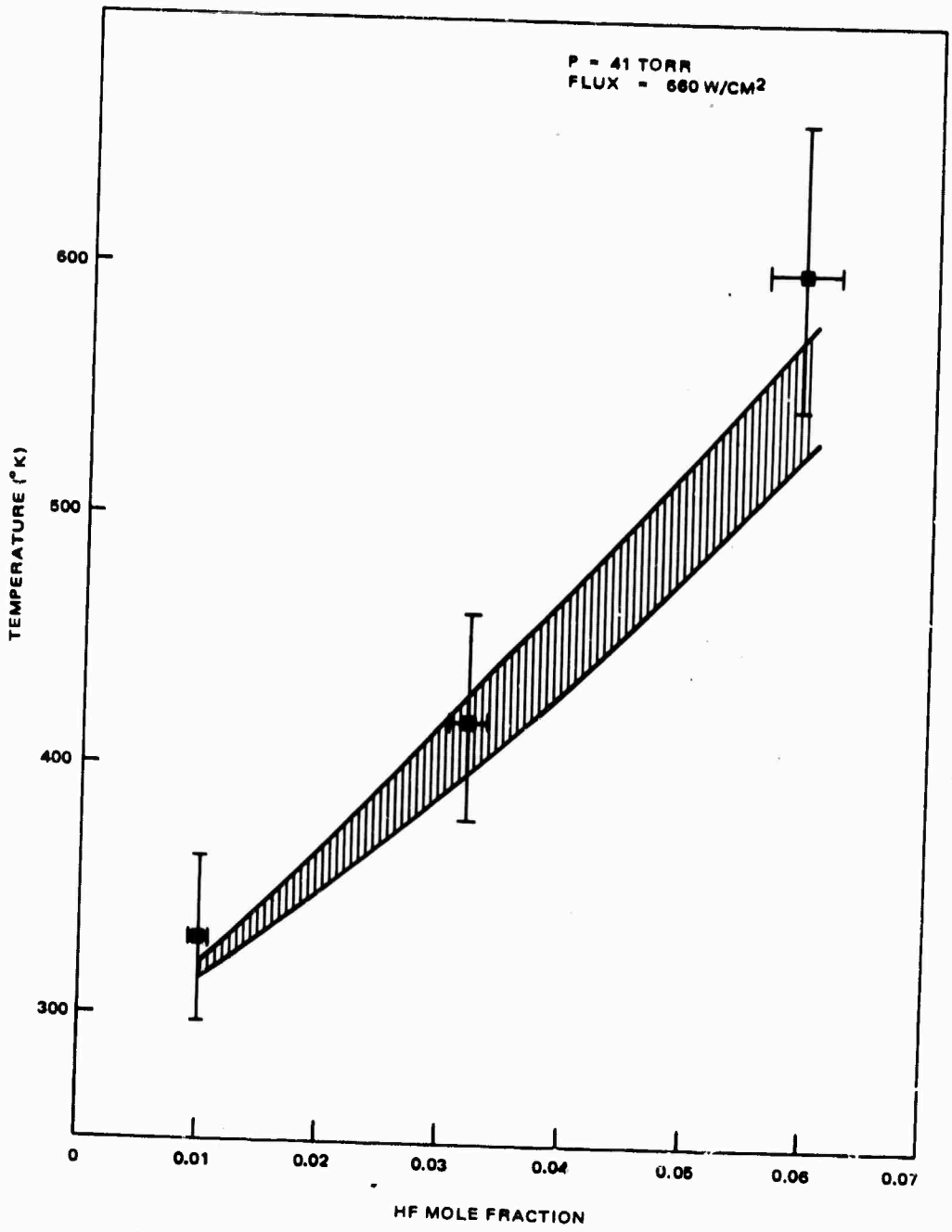

Figure 12. Optically pumped HF spectroscopic temperature (41 torr)

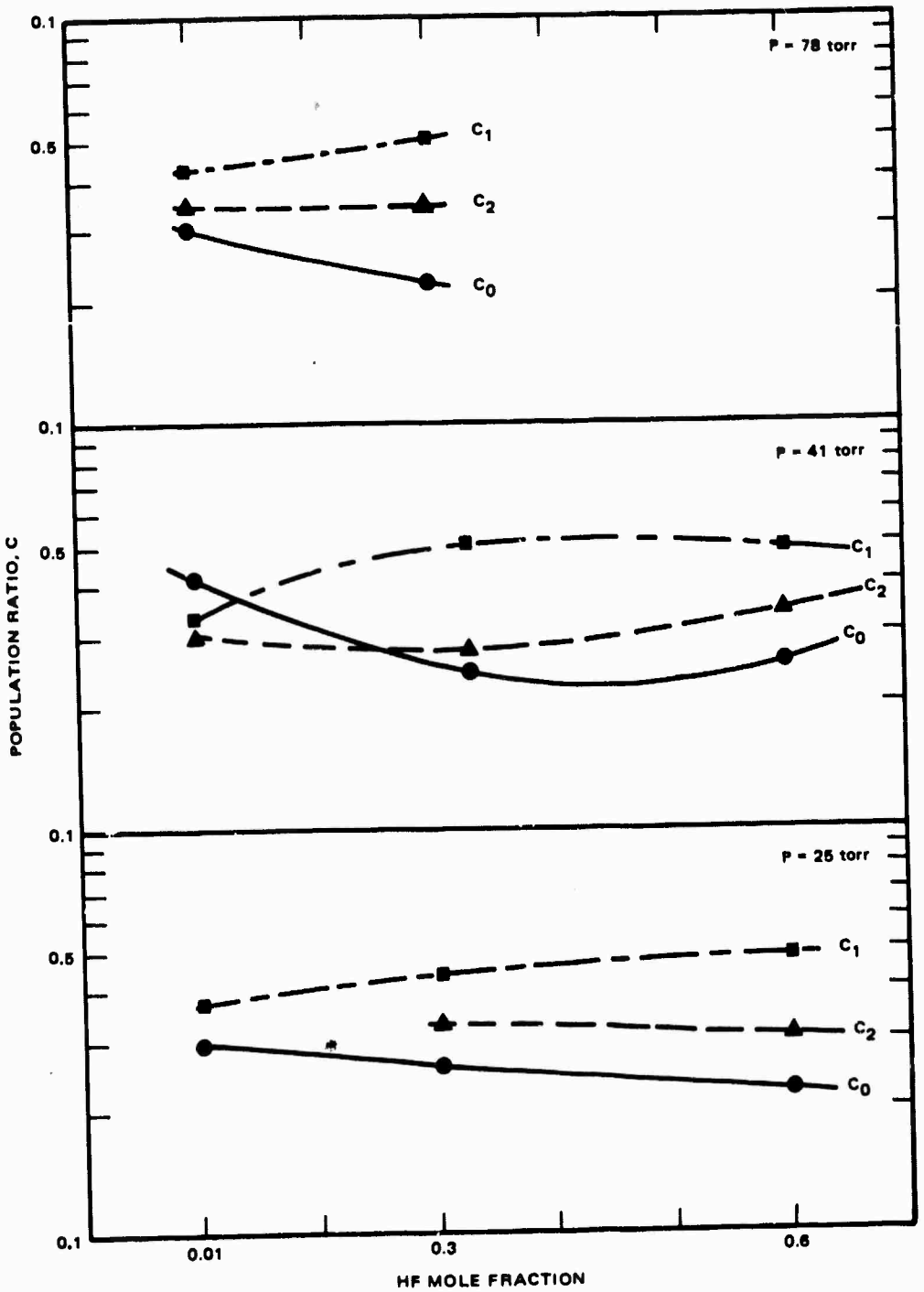

Figure 13. Optically pumped HF vibrational population ratios

A number of potential two-component ORTL candidate systems were also investigated. The acceptors and their mole fractions investigated are listed in Table 1. The pressure and pump irradiance were fixed at 41 torr and 3 kW/cm^2 respectively. The velocity was 5×10^3 cm/sec for all systems except HCN, where it was increased to 10^4 cm/sec because of the very rapid HCN self quenching rate. Fluorescence from both donor and acceptor was monitored during each experiment. Figures 14-17 illustrate typical emission spectra from the HF/HCl, HF/HBr, HF/HCN, and HF/DF systems.

In all the systems investigated the HF population ratios, C_0 and C_1, were approximately the same magnitude, and were constant with variation of acceptor mole fraction. This behavior is expected since C_0 and C_1 are regulated by the optical pump field. C_2 and the gas temperature at the interaction region do show variation for different acceptors. The HF population ratios shown in Figure 18 are exemplary of both HF/HCl and HF/HBr systems. Note that the temperature is constant throughout, and that C_2 gradually decreases with increasing acceptor mole fraction. However, C_2 rapidly decreases and the temperature rapidly increases with HCN mole fraction, as shown in Figure 19. This is also true for DF shown in Figure 20, but the trend is less rapid.

TABLE 1. ORTL MIXTURES INVESTIGATED IN FLUORESCENCE SCREENING EXPERIMENTS. The HF mole fraction was fixed at 3 percent and the diluent was helium.

Acceptor	Mole Fraction						
	1%	3%	6%	9%	11%	15%	18%
HCl	X	X		X			X
HBr		X		X		X	
DF	X	X		X			
HCN	X	X	X	X	X		

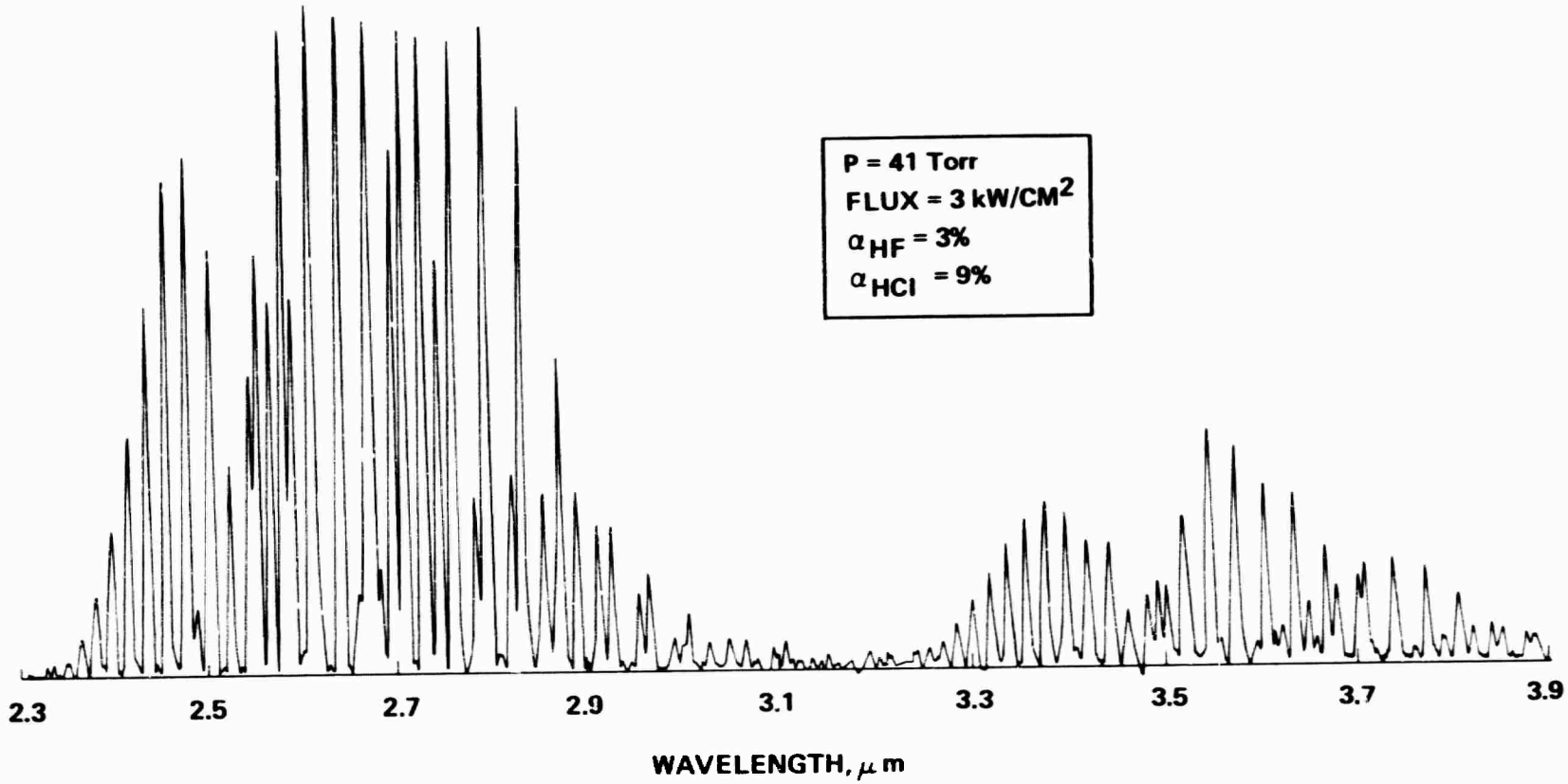

Figure 14. HF/HCl emission spectrum

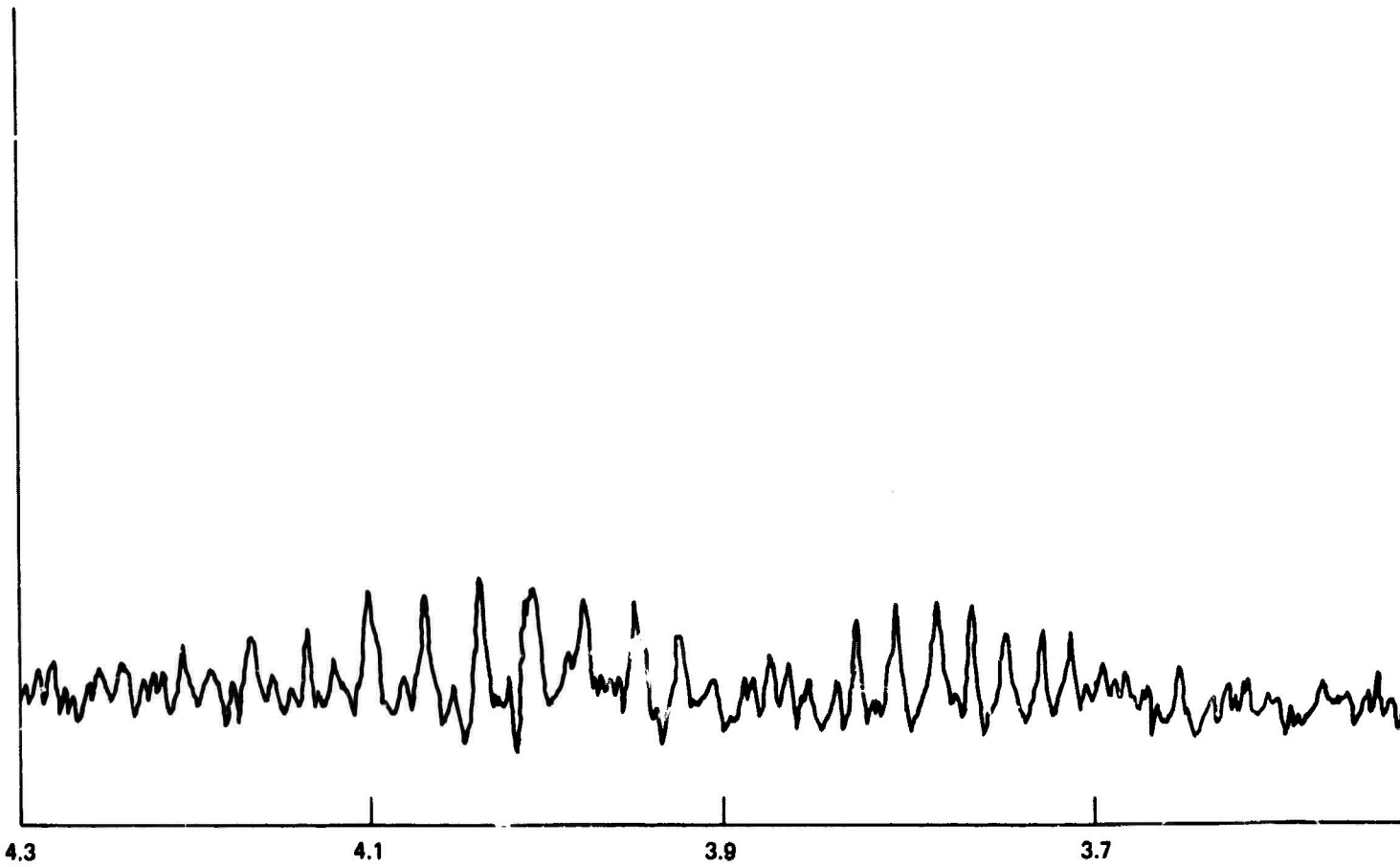
4.3
4.1
3.9
3.7

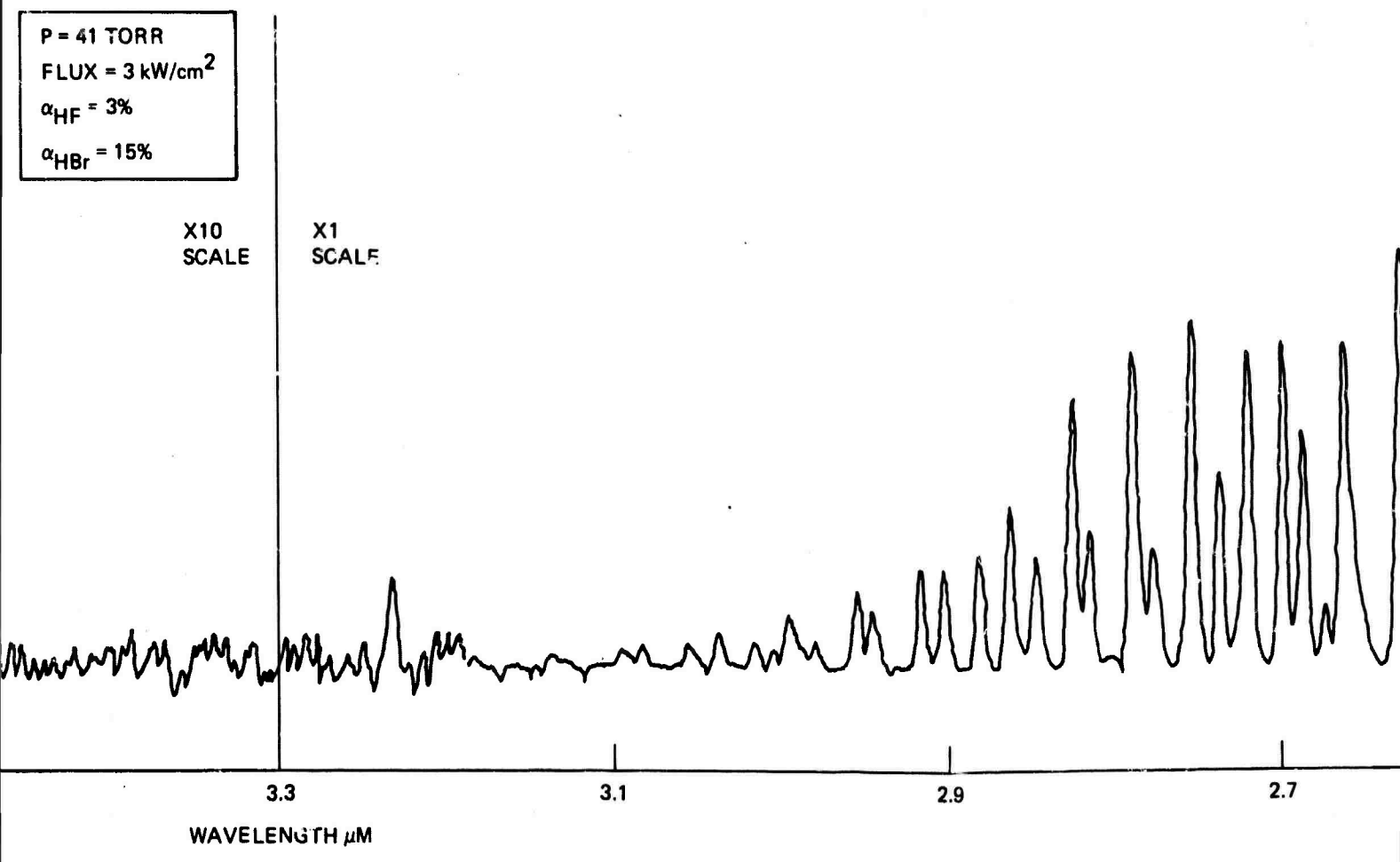
P = 41 TORR
FLUX = 3 kW/cm^2
α_{HF} = 3%
α_{HBr} = 15%
X10 SCALE
X1 SCALE
3.3
3.1
2.9
2.7
WAVELENGTH μM

2

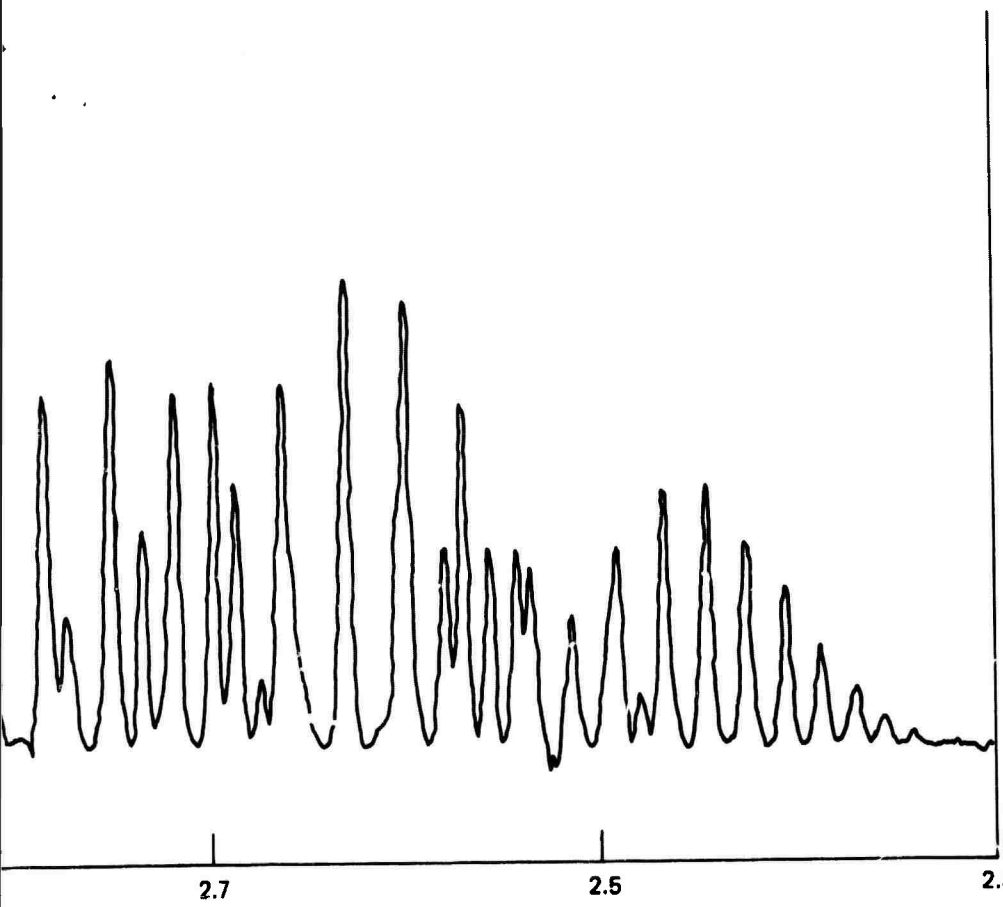

Figure 15. HF/HBr emission spectrum

3

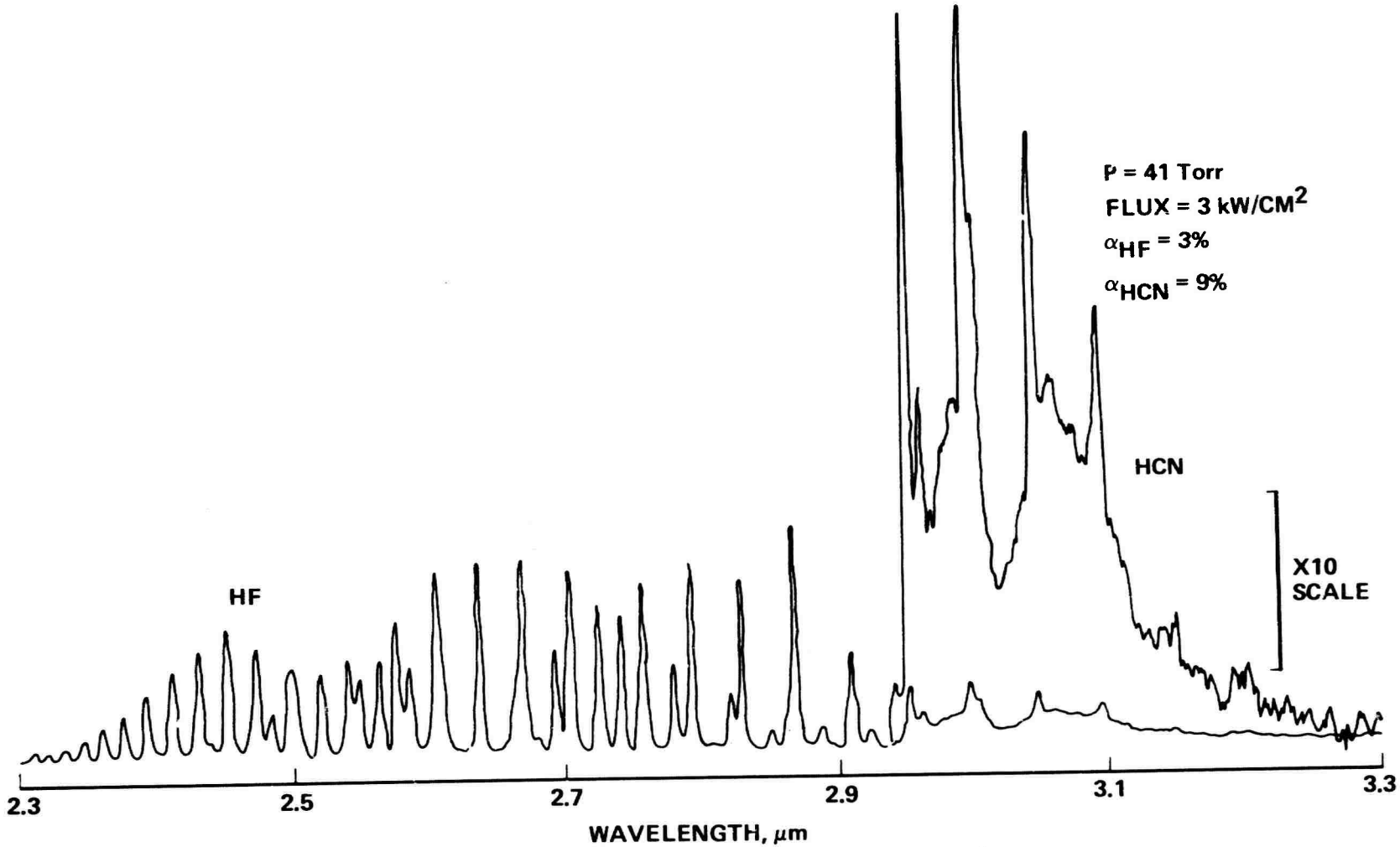

Figure 16. HF/HCN emission spectrum

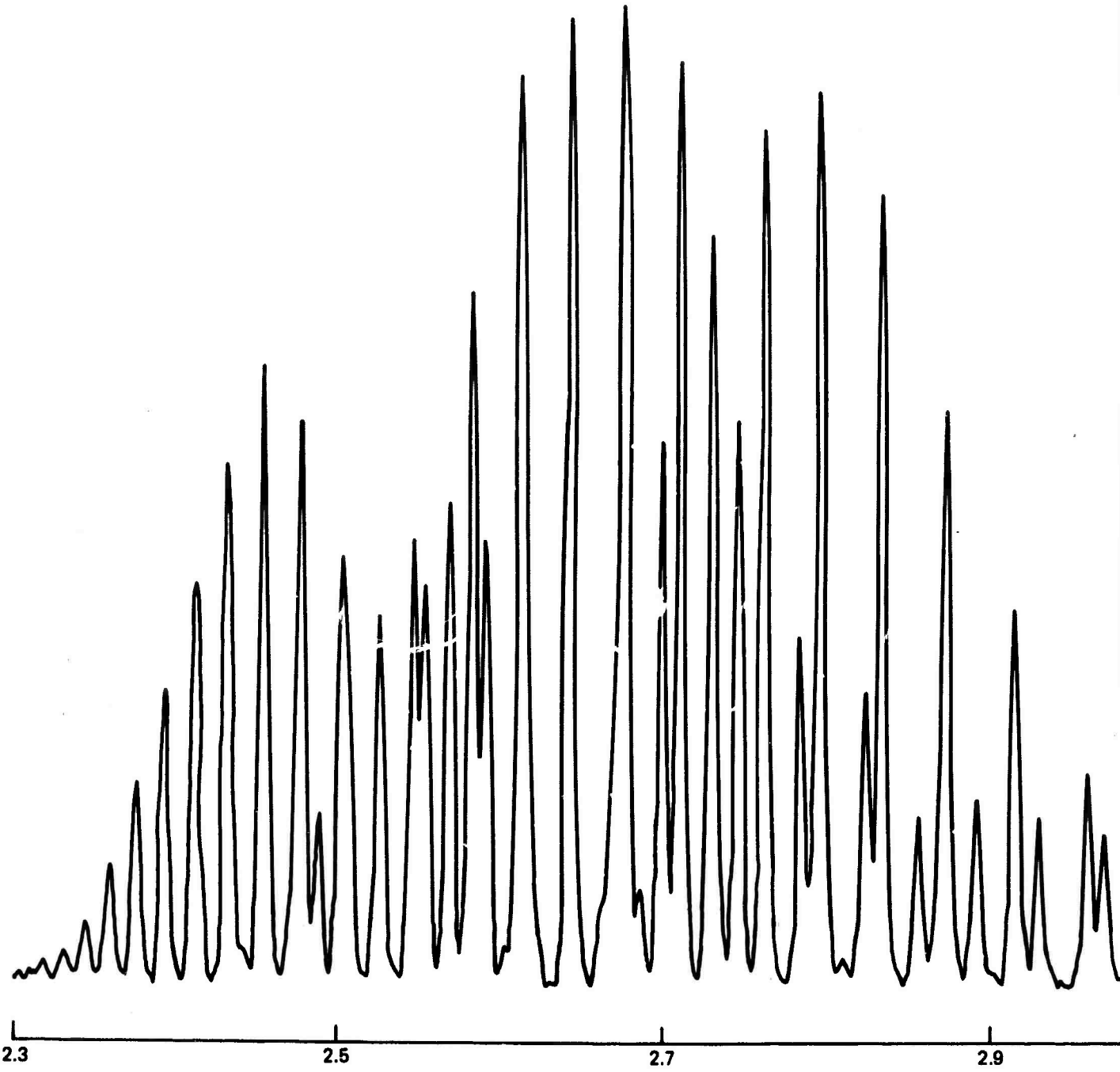
2.3
2.5
2.7
2.9

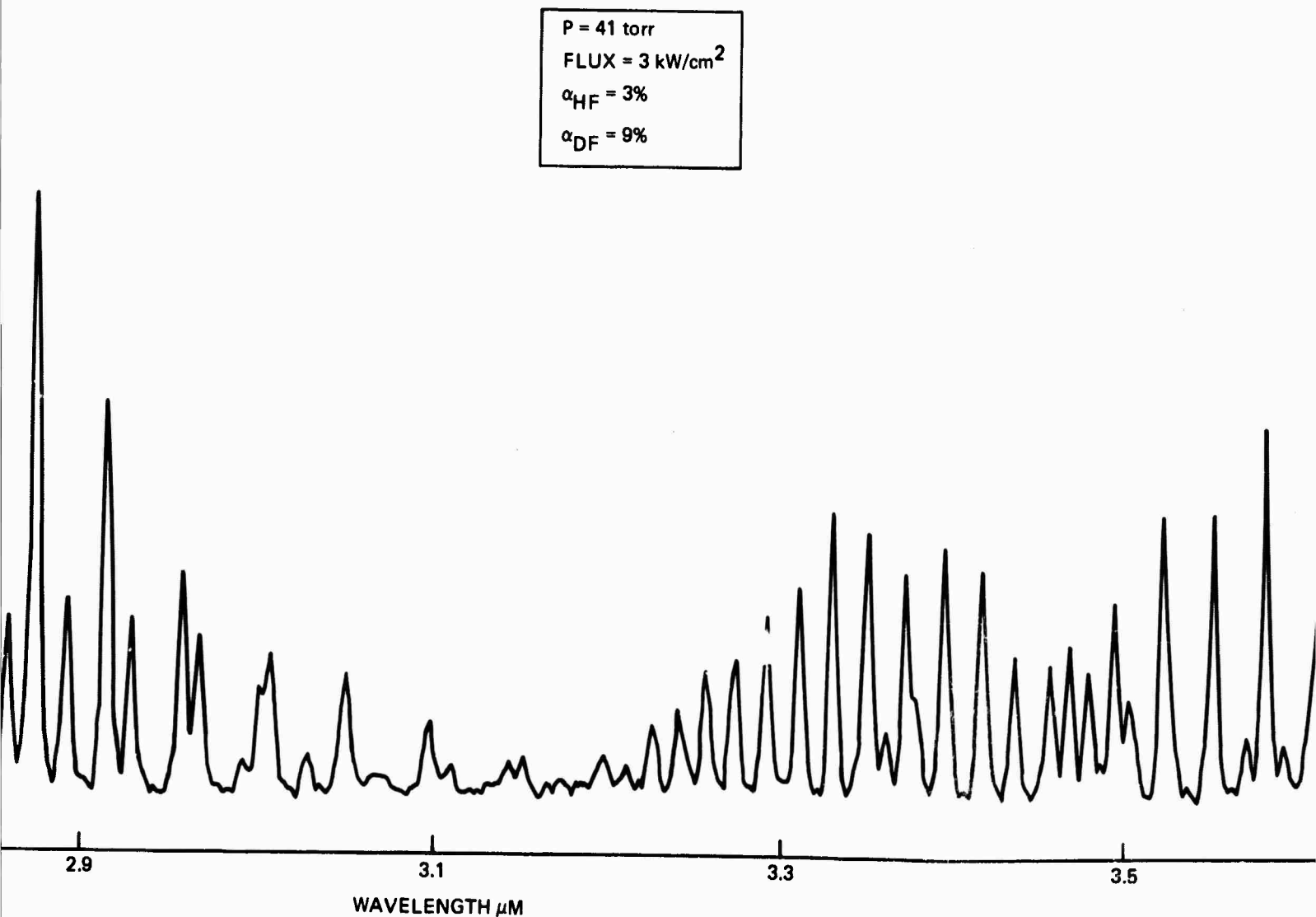
P = 41 torr
FLUX = 3 kW/cm^2
α_{HF} = 3%
α_{DF} = 9%
2.9
3.1
3.3
3.5
WAVELENGTH μM

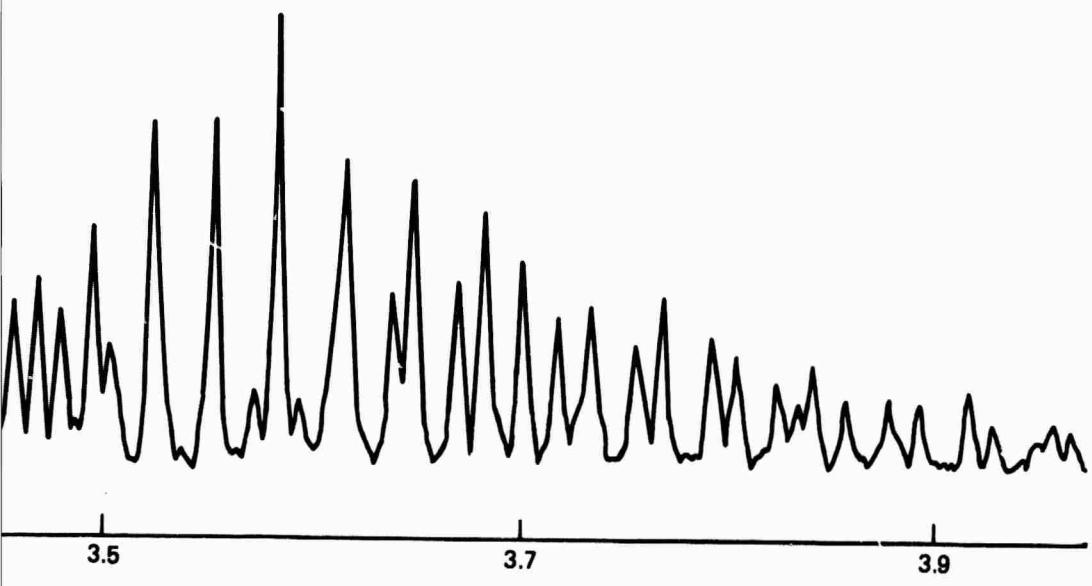

Figure 17. HF/DF emission spectrum

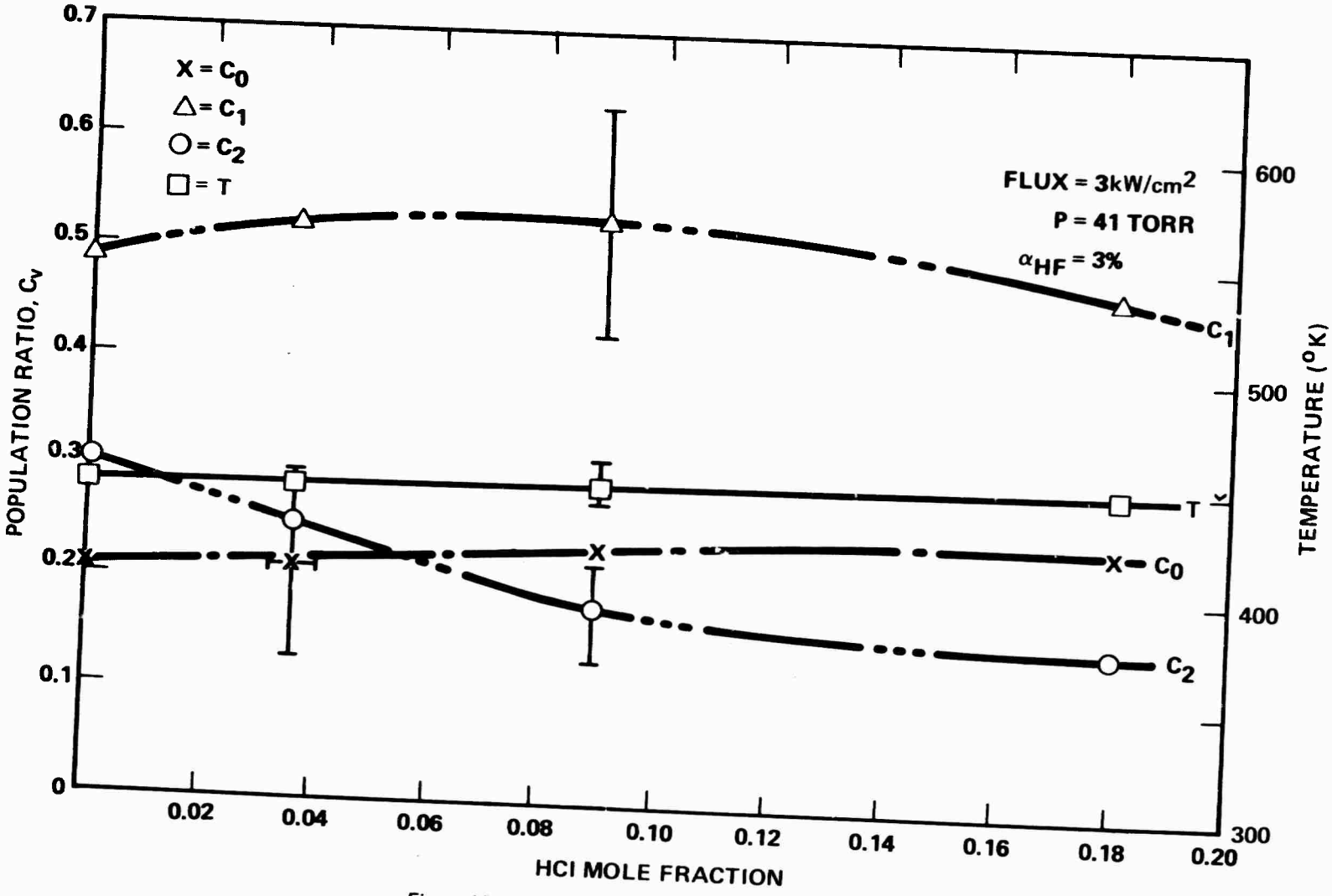

Figure 18. HF population ratios in the HF/HCl system

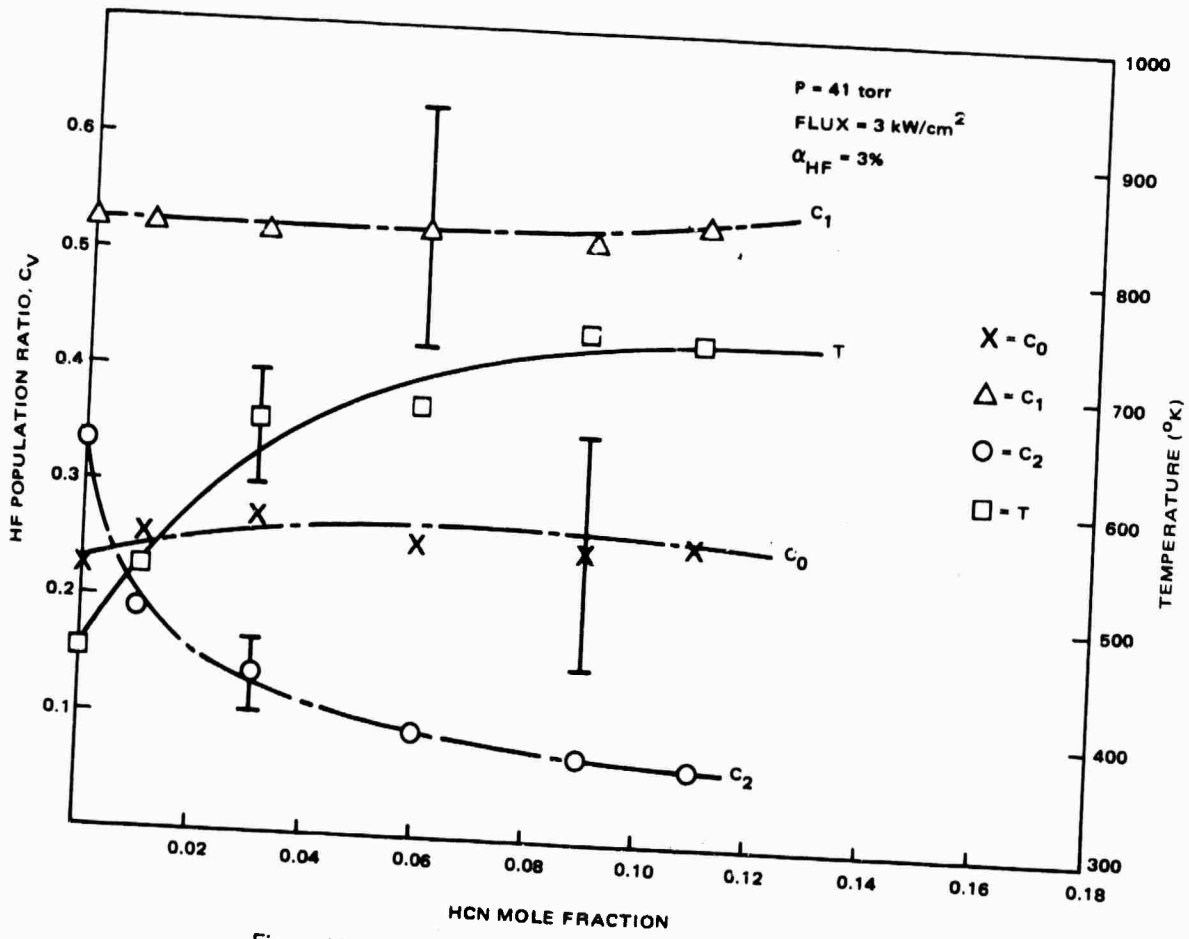

Figure 19. HF population ratios in the HF/HCN system

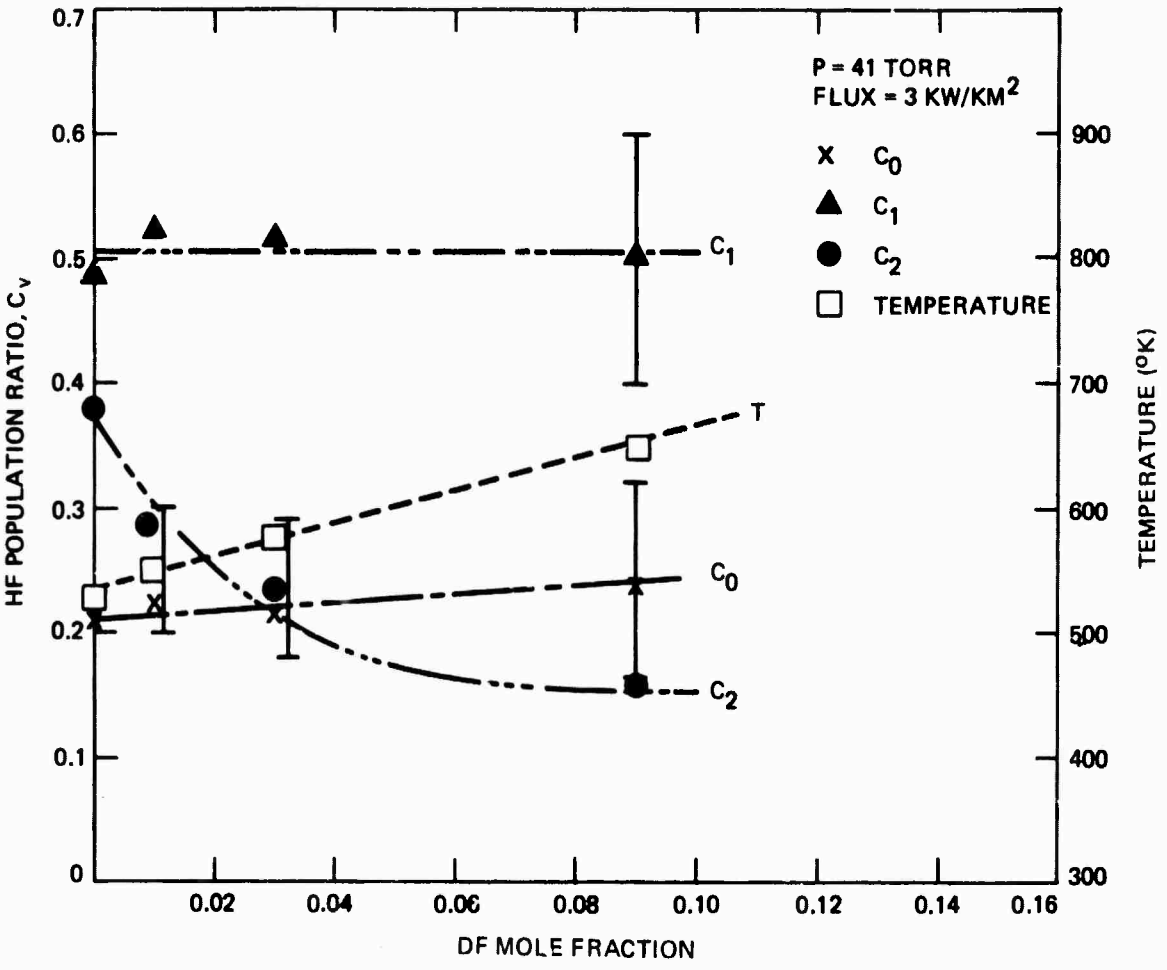

Figure 20. HF population ratios in the HF/DF system

These trends may be understood with reference to the kinetic processes that affect C_2 and the temperature. The HF v = 3 level is populated through HF V-V exchange in competition with energy transfer to the acceptor and depopulated primarily energy transfer to the acceptor. For HCl (or HBr) the transfer rate is 34 times (or 9) times slower than the HF V-V exchange rate. Therefore additions of HCl or HBr deplete the HF v = 3 population weakly. For HCN the transfer rate is only 3 times slower; this process is therefore more important and there is a strong dependence of C_2 on HCN mole fraction. The DF rate is intermediate between those for HCN and HCl

being 7 times slower than the HF exchange rate. This is still fast enough to be important. On the other hand, the temperature is governed by the self quenching rate of the HF and acceptor molecules. Relative to HF self quenching, the self quenching rates of HBr, HCl, DF, and HCN are slower by a factor of 100, 80, 3, and 1 respectively. Therefore the temperature in the first two systems is unaffected by an increase in the acceptor concentration, while in the other two systems it increases with additional acceptor concentration.

The variation of acceptor population ratios $\overline{C}_v$ with mole fraction for HBr and HCN are shown in Figure 21, for HCl in Figure 22 and for DF in Figure 23. With reference to the figures, the $\overline{C}_v$ values for all acceptors are less than the corresponding values for HF. Consequently in terms of a lasing demonstration experiment, the HF system is the most favorable one. The HF/DF system with $\overline{C}_1$ values near 0.4 also appears to be a viable candidate, while HF/HCl does not appear to be as good, and the HF/HBr and HF/HCN (3.1 μ) systems are not promising candidates.

2.7 LASER DEMONSTRATION EXPERIMENTS

The systems investigated in this phase were optically pumped HF (2.7 to 3.1 μ), and the HF/DF (3.7 to 4.2 μ), HF/HCl (3.7 to 4.1 μ), and HF/HCN (3.8 - 3.9 μ)* ORTL systems. The apparatus used in the laser demonstration experiments was almost identical to that used in the fluorescence experiments except that an ORTL resonator consisting of two mirrors was aligned along the 6 cm gain medium direction. A schematic diagram was shown in Figure 5. A 1.2 x 2.3 cm chemical laser beam was cylindrically focused to 0.38 x 2.3 cm in the ORTL cell containing a 0.3 x 6 cm nozzle. The nozzle was rotated at a 20 degree angle so that the 2.3 cm pump beam could pump the entire 6 cm length of the ORTL flow. A backup mirror returned the transmitted pump beam back through the ORTL medium to enhance the pumping flux.

Three ORTL resonators were used in the laser demonstration attempts. The first resonator was a closed cavity consisting of a 99.5 percent

*See Figure 32.

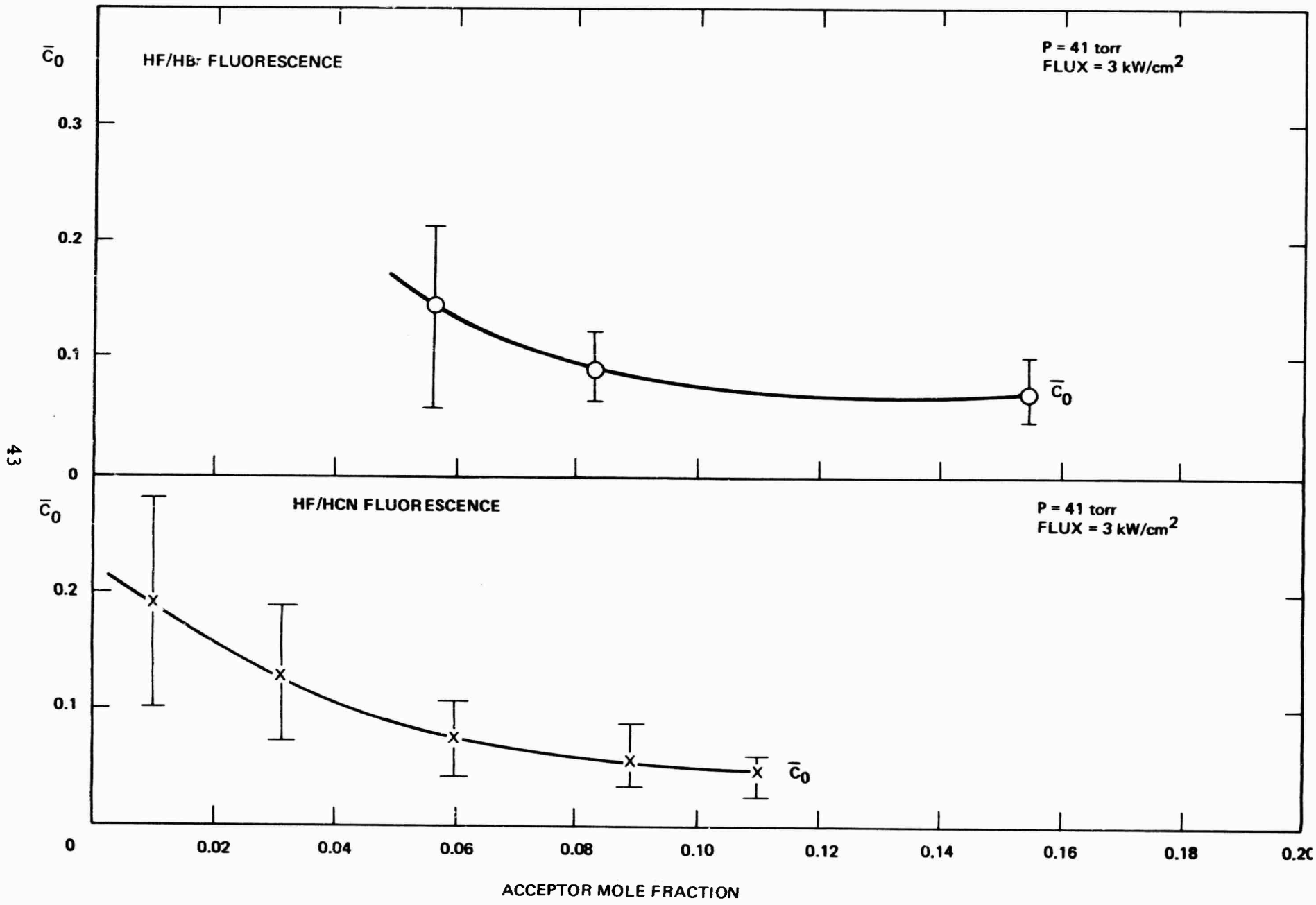

Figure 21. HCN and HBr vibrational population ratios in the HF/HCN and HF/HBr systems

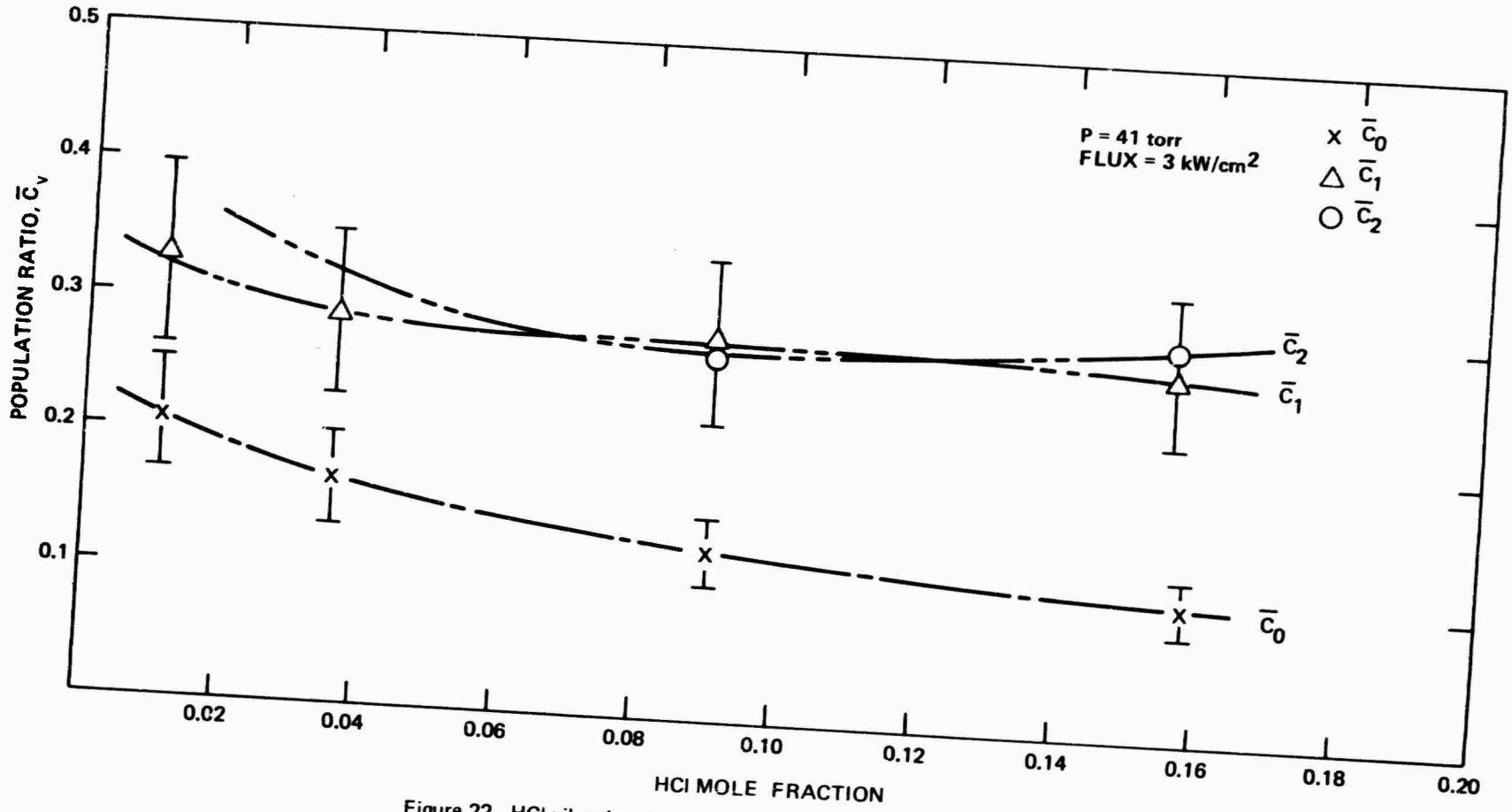

Figure 22. HCl vibrational population ratios in the HF/HCl system

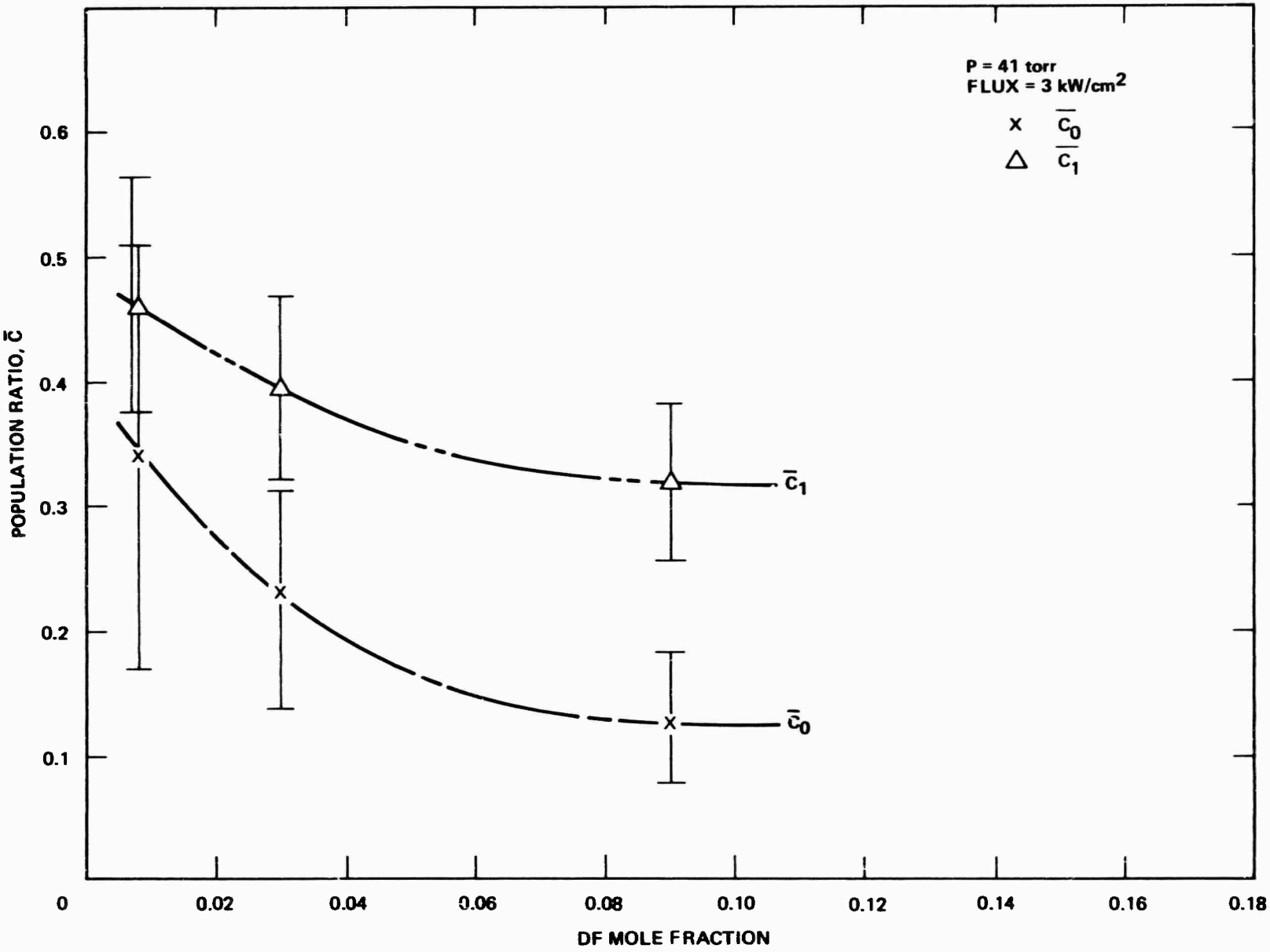

Figure 23. DF vibrational population ratios in the HF/DF system

reflecting flat and a 99.5 percent reflecting mirror with a 3 meter radius of curvature. The total round trip loss was 1 percent in the 3.4 to 4.1 μ range and 30 percent in the 2.7 to 2.9 μ range. In the second resonator, the curved mirror was replaced by a 1.2 percent transmission outcoupler with a total loss of 2 percent in the 3.4 to 4.1 μ range. In the third resonator, a 5 percent transmission outcoupler with a total loss of 7 percent in the 2.7 to 2.9 μ ramge was used. The threshold gains required to sustain laser oscillation for these three resonators were 8.3×10^{-4}/cm, 1.7×10^{-3}/cm and 5.8×10^{-3}/cm, respectively. The transmittances and the reflectances of these mirrors were measured on a double beam spectrophotometer with expanded scale capability. Mirror separation was approximately 75 cm for all tests.

The predicted gain for each candidate two level system derived from the data in the fluorescence experiments taking into account the kinetic rate uncertainties is shown in Figure 24 along with the threshold gains for the various resonators. For the optically pumped HF system, the estimated round trip gain with 3 percent HF is between approximately 12 percent and 85 percent so the 5 percent outcoupling resonator was chosen for a laser demonstration attempt. In the other systems the estimated round trip gains were between 0.1 percent and 3 percent. Therefore, the lasing attempts for these systems were first performed with the closed cavity resonator. After lasing was observed in a particular system, the 1.2 percent outcoupling resonator was used for outcoupled power measurement. A scanning spectrometer was used to monitor the scattered ORTL light from one of the resonator mirrors. This spectrometer data was used to assign the lasing transitions and to detect laser oscillation in the closed cavity resonator.

In almost all lasing experiments with the optically pumped HF system the 5 percent outcoupling ORTL resonator was used. The gas velocity was maintained at 5×10^3 cm/sec. Three series of experiments were performed. The first two series were performed at 28, 41, and 78 torr with several different HF mole fractions at each pressure. The pump laser with $\beta_{\Delta F_2} = 0.067$ and $\beta_{\Delta F_2} = 0.042$ was used in these two series. Output powers as a function of the HF mole fraction are shown in Figure 25a and 25b. The pump laser with lower power (380 watts pump laser) yielded higher output powers. As

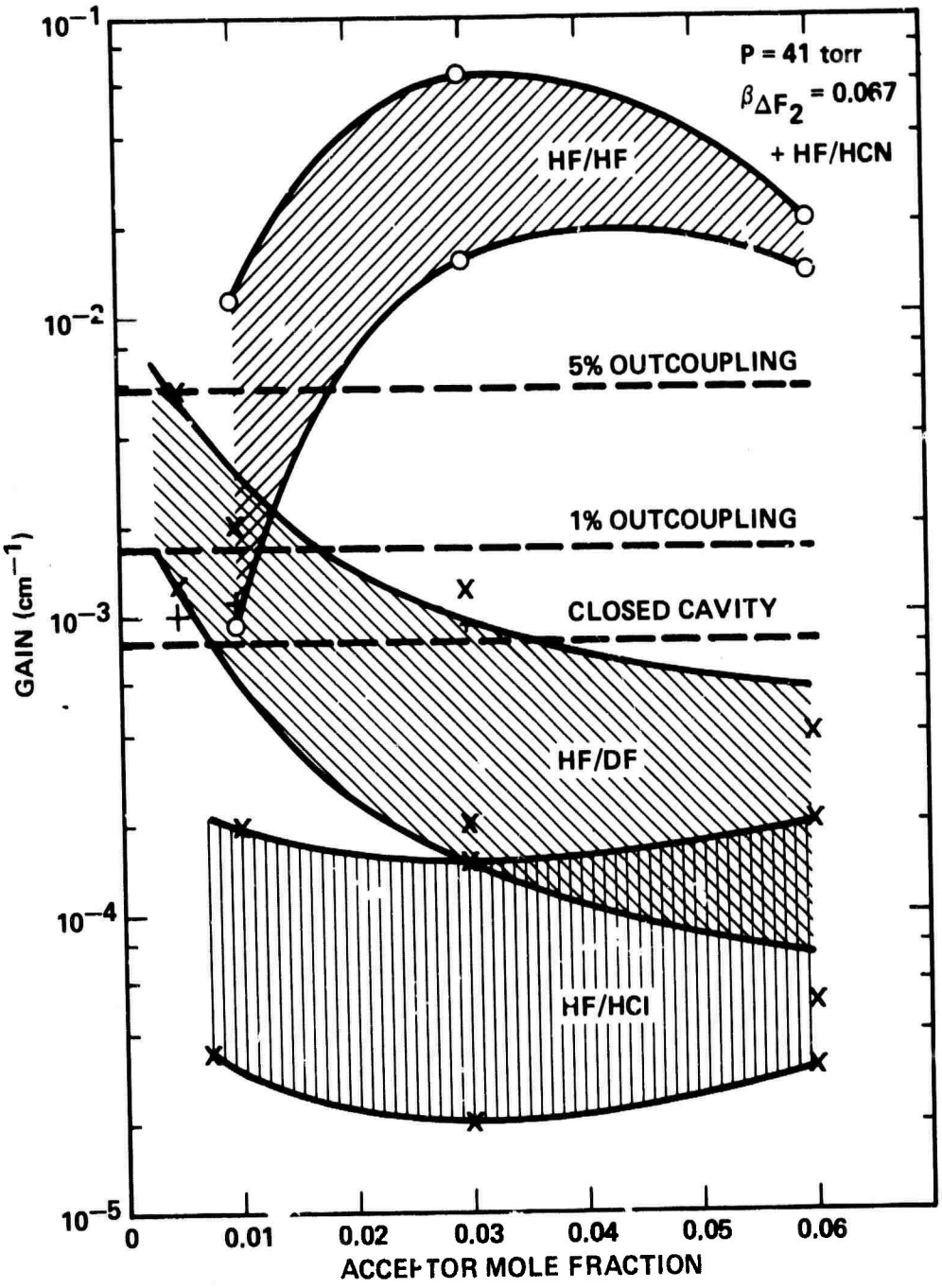

Figure 24. Small signal gain calculations for different systems

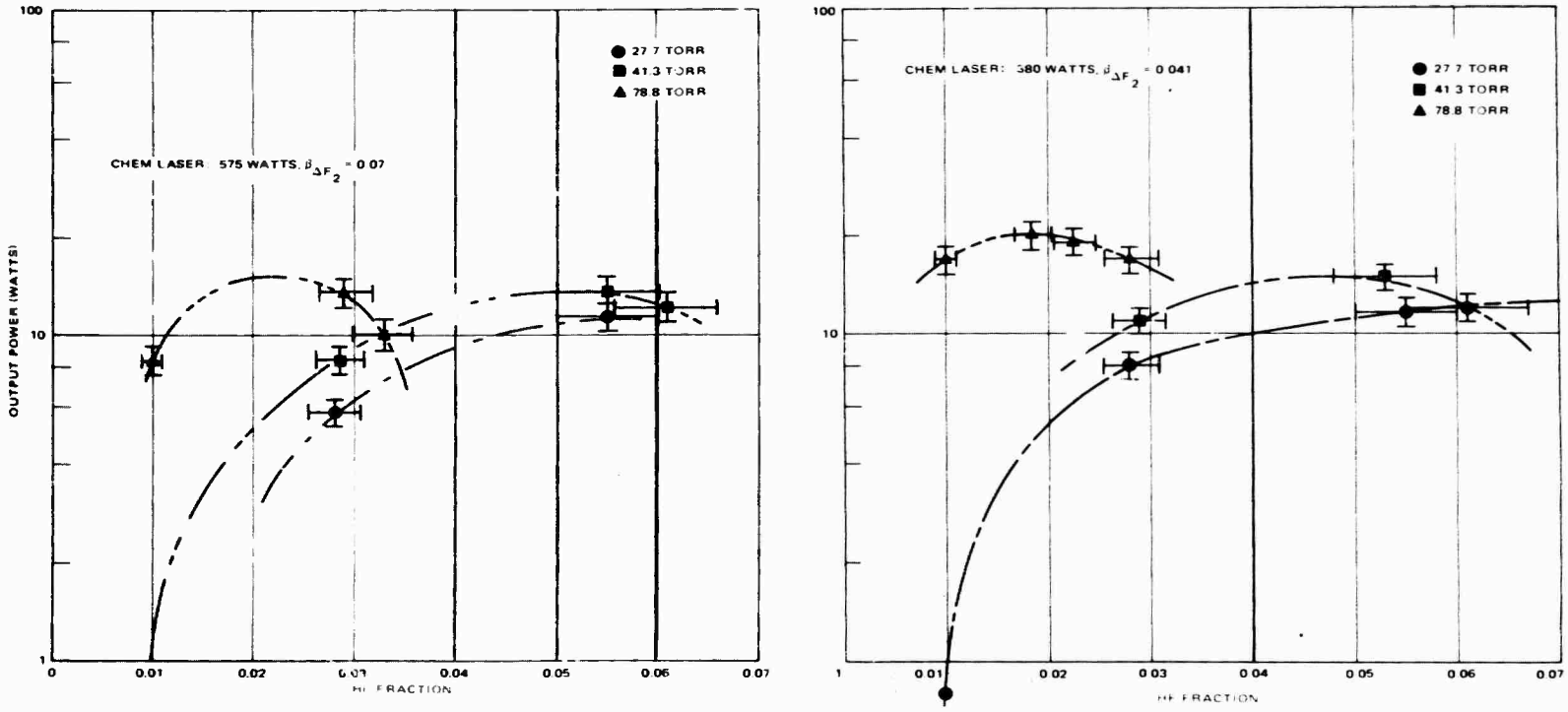

Figure 25. Optically pumped HF laser output power

discussed earlier, this was expected. The output performance was better at higher gas pressure in each series. A maximum of 20.2 watts of outcoupled power was observed at 78.8 torr with 1.8 percent HF. This corresponds to a 5.3 percent overall conversion efficiency of incident pump laser power to outcoupled ORTL power. The spectral distributions of the output power were not monitored in these two series.

In order to evaluate the performance of the optically pumped HF laser more adequately, both the outcoupled power and laser output spectrum were measured in a third series of experiments. This series of experiments was performed at 78 torr with 2 percent HF and at 110 torr with 1 percent and 2 percent HF, in an attempt to obtain better performance. Output data are shown in Figure 26. Note that at 78 torr and 2 percent HF, the outcoupled 11 watts was only half of that observed in the previous series. Since the emphasis in the Screening Task was on laser demonstration, no attempt was

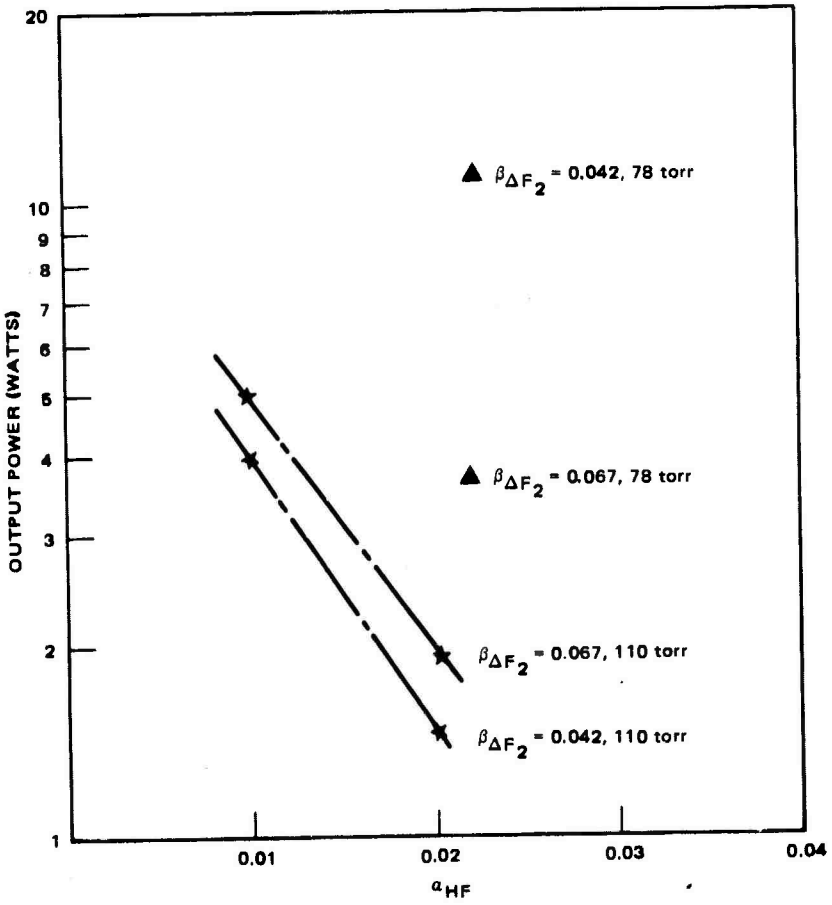

Figure 26. Optically pumped HF laser output powers – 78 and 110 torr

made to optimize the experimental conditions (the output performance) in this third series. The important information from this series is that the outputs at 110 torr were less than the outputs at 78 torr. The pump laser probably was not strong enough to sustain the same degree of population inversion at high pressure conditions. For the three cases in the third series for which the output spectrum was monitored, the power was distributed among the $P_1(9)$, $P_1(10)$, $P_2(8)$, and $P_2(9)$ lines with most power concentrated on the $P_2(8)$ transition. In some cases, oscillation on the $P_1(8)$ transition was also observed. The output spectral distribution for the case of 78 torr with 2 percent HF is illustrated in Figure 27. Seventy-eight percent of the power is in the $P_2(8)$ line. For these experiments, no line selection was attempted; the resonator mirror reflectivities were flat over the lasing wavelength range. Thus, single-line efficiencies with line selection should be greater than 78 percent of the efficiencies observed in the present series of experiments.

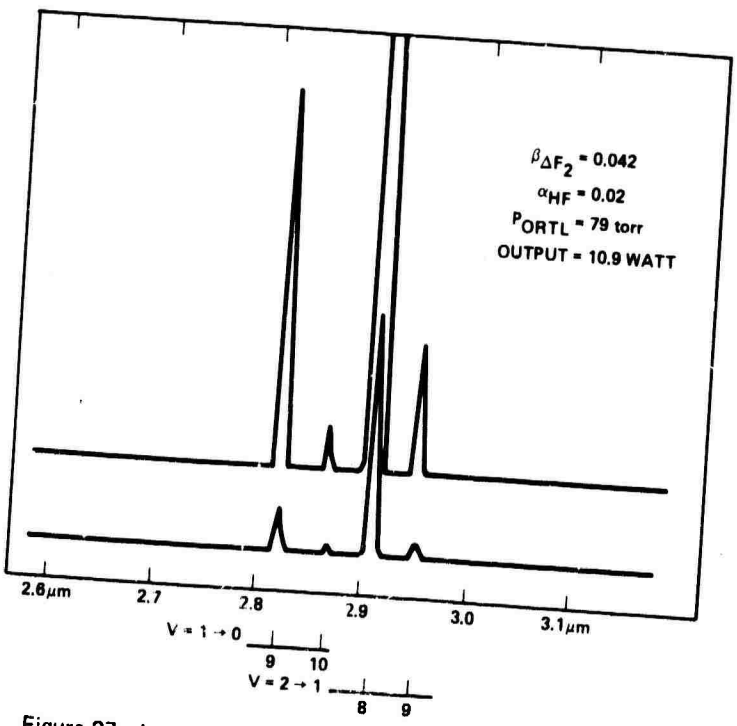

Figure 27. Laser spectrum for the optically pumped HF system

Optically pumped HF lasing was also observed at 41 torr with 3 percent HF with a different closed cavity resonator for which the reflectivities at HF wavelengths were much lower. This resonator had a round trip loss of 30 percent at the HF lasing wavelength, indicating that the small signal gain in this experiment was greater than 3 percent per centimeter. This high value is consistent with the estimates in Figure 24.

The ORTL system efficiency is described by the product of three terms. The input coupling efficiency η_i, is the fraction of the HF power absorbed

$$\eta_i = \frac{\text{power absorbed}}{\text{available pumping power}}$$

The power conversion efficiency η_{conv}, is the fraction of absorbed power converted to coherent ORTL power

$$\eta_{conv} = \frac{\text{coherent ORTL power}}{\text{power absorbed}} = \frac{\text{output + cavity loss}}{\text{gas heating + output + cavity loss}}$$

The outcoupling efficiency η_{out}, is the fraction of power outcoupled from the ORTL resonator

$$\eta_{out} = \frac{\text{output}}{\text{output + cavity loss}}$$

The overall efficiency η_T, is simply the product of these three components

$$\eta_T = \frac{\text{output}}{\text{available pumping power}} = \eta_i \cdot \eta_{conv} \cdot \eta_{out}$$

The relative value of the output power and the total coherent power can be obtained by delineating all losses of the ORTL resonator components. For example, the 5 percent outcoupling resonator had a total loss (including mirror losses) of 7 percent, thus $\eta_{out} = 0.71$. One can then determine the total coherent ORTL power from this output efficiency together with the outcoupled power measurement.

The heat generated in the ORTL gas, $\dot{Q}$, can be obtained from

$$\dot{Q} = \overline{C}_p \cdot \Delta T \cdot \dot{Z}$$

where $\overline{C}_p$ is the average specific heat, ΔT the temperature rise in the gas and $\dot{Z}$ the molar flow rate of the ORTL gas. The temperature rise was measured by a thermocouple placed 1.2 cm downstream of the pump interaction zone. Combining $\dot{Q}$ and the total coherent power, one can easily calculate the conversion efficiency, η_{conv}, and the input efficiency, η_i.

The overall efficiencies are shown in Figure 28 for the series with the $\beta_{\Delta F_2} = 0.042$ pump laser. Results from computer model calculations are shown by the dotted lines in this figure. They are fairly close to the experimental values in the high pressure case (78 torr) but tend to differ in

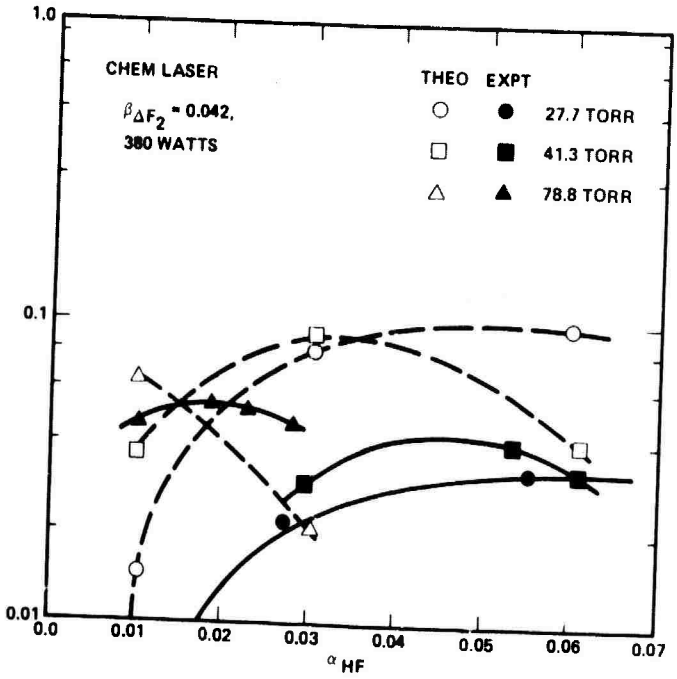

Figure 28. Overall efficiency for the optically pumped HF system

the low pressure cases. Since rotational equilibrium is assumed in the model, the deviation may be due to rotational non-equilibrium at low pressure.

In this task no attempt at optimizing efficiency was made. The input coupling efficiency could be improved by increasing the optical pumping length or by implementing a more optimum configuration. The conversion efficiency, however, is limited by the nature of the physics in the system, and is a critical parameter for determining eventually achievable overall efficiencies. The conversion efficiencies for the 78 torr data of Figure 28 are shown in Figure 29, together with the computer model predictions. The best achieved conversion efficiency was 34.5 percent at a 1.0 percent HF mole fraction. Note that the best overall efficiency, 5.3 percent, was achieved at a 1.8 percent HF mole fraction. The predicted values agree fairly well with the experimental results. Also illustrated in this figure are the predicted results for conditions with a much higher pumping flux, 3.1 kW/cm^2. These indicate that 80 to 85 percent conversion efficiencies may be achievable. A summary of the measured efficiencies at 78 torr is shown in Table 2.

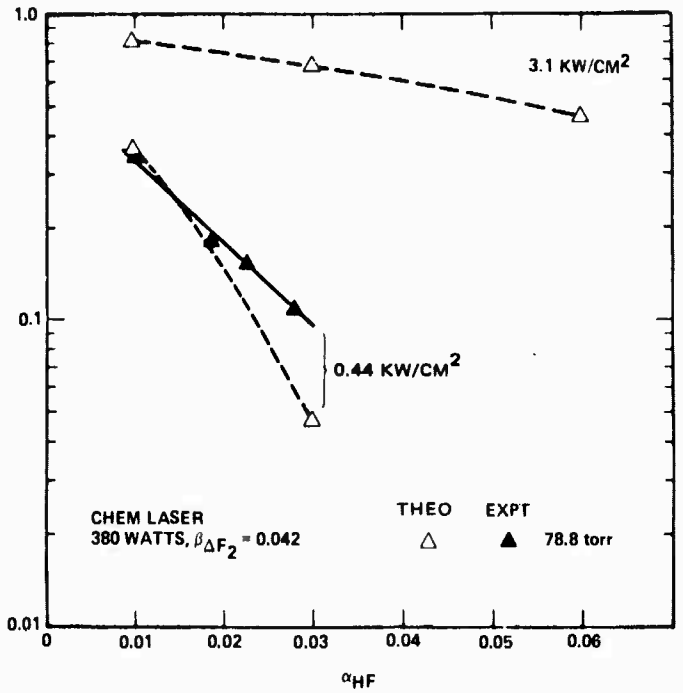

Figure 29. Power conversion efficiency for the optically pumped HF system

TABLE 2. OPTICALLY PUMPED HF LASER EFFICIENCIES MEASURED AT 78 TORR

Series	β_{HF}	Output (watts)	η_i	η_{conv}	η_T
		$\beta_{\Delta F_2}$ = 0.067, 575 watt pump laser			
I	0.01	8.2	0.102	0.198	0.014
I	0.029	13.6	0.419	0.080	0.024
I	0.033	10.0	0.501	0.049	0.017
III	0.0214	4.0	0.274	0.036	0.007
		$\beta_{\Delta F_2}$ = 0.042, 380 watt pump laser			
II	0.01	16.8	0.182	0.345	0.044
II	0.0185	20.2	0.407	0.181	0.053
II	0.0226	18.8	0.450	0.156	0.049
II	0.028	16.8	0.586	0.112	0.044
III	0.020	10.9	0.344	0.078	0.029

The most significant results with the optically pumped HF laser include:

- Maximum output of 20.2 watts
- Maximum small signal gain of greater than 3 percent per centimeter
- Maximum conversion efficiency of 34.5 percent
- Maximum lasing pressure of 110 torr
- 78 percent of output concentrated on a single line (with no line selecting elements).

Analysis of the two component fluorescence data indicated that the HF/DF ORTL system could successfully be demonstrated with the available laboratory apparatus. It also indicated that the HF/HCl system might lase and the HF/HCN could lase to levels other than the ground state. Therefore, lasing demonstration experiments were undertaken for these three systems.

The closed cavity resonator with 1 percent round trip loss was used for the initial laser demonstration attempts. After laser oscillation was demonstrated in a system, the 1.2 percent outcoupling resonator was used for output power measurement. The experimental operating conditions and the test results with the closed cavity resonator are summarized in Table 3. The HF mole fraction was set at 3 percent and the acceptor mole fraction was varied from 0.5 percent to 6 percent. A gas velocity of 5×10^3 cm/sec was selected for most systems except the HF/HCN where 1×10^4 cm/sec was used. The spectrometer to collect the scattered ORTL light was scanned over the 2.6 to 4.3 μ range to monitor both the donor (HF) and the acceptor lasing transitions.

No HCl laser oscillation was observed with the HF/HCl system. In the HF/DF system, oscillation to the ground state was observed only in the case of 0.5 percent DF mole fraction. Subsequently, 25 milliwatts was outcoupled using the 1.2 percent outcoupling resonator. Oscillation was observed on the $P_1(11)$, $P_1(12)$, $P_1(13)$, $P_2(11)$, and $P_2(12)$ lines as shown in Figure 30. No lasing was observed when the DF mole fraction was increased. Lasing with only small acceptor mole fraction relative to the donor mole fraction was expected (see Figure 24).

TABLE 3. ORTL LASER DEMONSTRATION EXPERIMENTS

- ORTL Resonator: Closed Cavity
- Velocity: 5×10^3 cm/sec (HCN 10^4 cm/sec)
- Pressure: 41 torr
- HF Mole Fraction: 3%

Was Laser Oscillation Observed?

Acceptor Mole Fraction	Acceptor		
	HF/DF	HF/HCl	HF/HCN
0.5%	Yes	No	Yes
1%	No	No	Yes
3%	No	No	Yes
6%	No	No	No

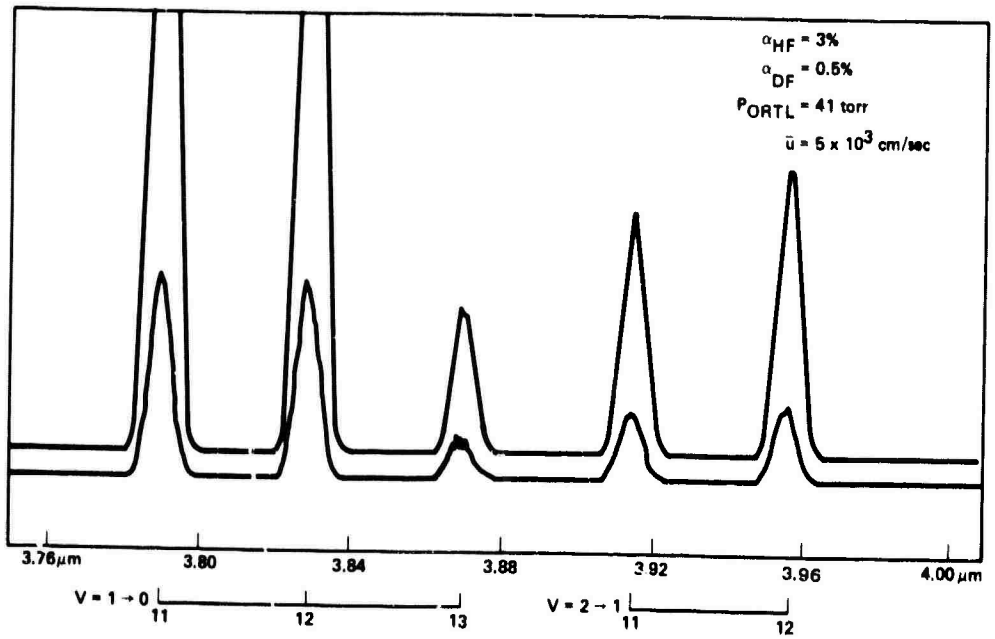

Figure 30. HF/DF ORTL spectrum

Laser oscillation was also observed in the HF/HCN system with 0.5 percent, 1 percent and 3 percent HCN mole fractions. However, oscillation was achieved only with the closed cavity resonator and attempts with the 1.2 percent outcoupling resonator were unsuccessful. This indicated that the gain was between 8.3×10^{-4} and 1.7×10^{-3} per centimeter. The output spectra for two different HCN mole fractions are shown in Figure 31. Looking at the energy levels shown in Figure 32, the 3.85 μ lasing with 0.5 percent HCN is the $(00^01) \rightarrow (01^10)$ transition and the 3.90 μ line in the 3.0 percent HCN case is the $(01^11) \rightarrow (02^20)$ transition. In the latter case, the higher HCN concentration caused the gas temperature to raise high enough to populate the (01^10) state thermally. Thus, the lasing on the $(00^01) \rightarrow (01^10)$ transition was terminated and it forced the system to lase on the $(01^11) \rightarrow (02^20)$ transition.

Highlights of the successful laser demonstration experiments are summarized in Table 4. For the two component ORTL systems which were investigated on this program, the most efficient system was HF/DF.

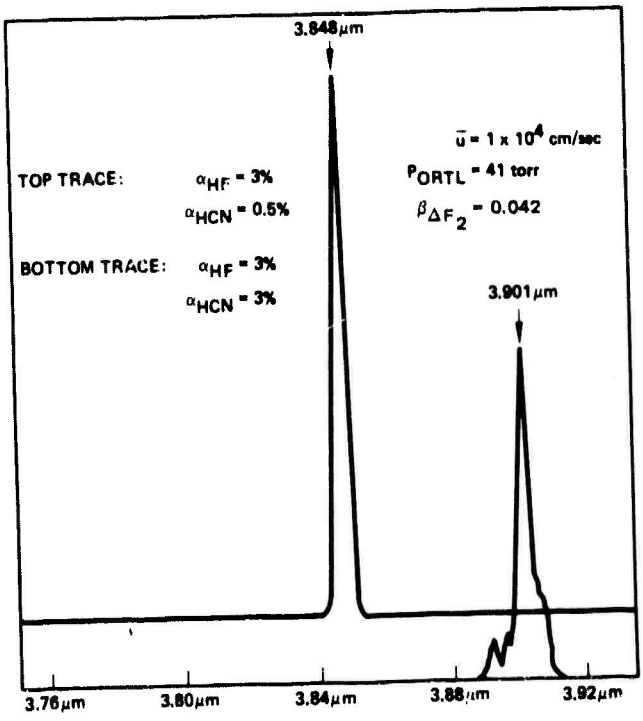

Figure 31. HF/HCN ORTL spectra

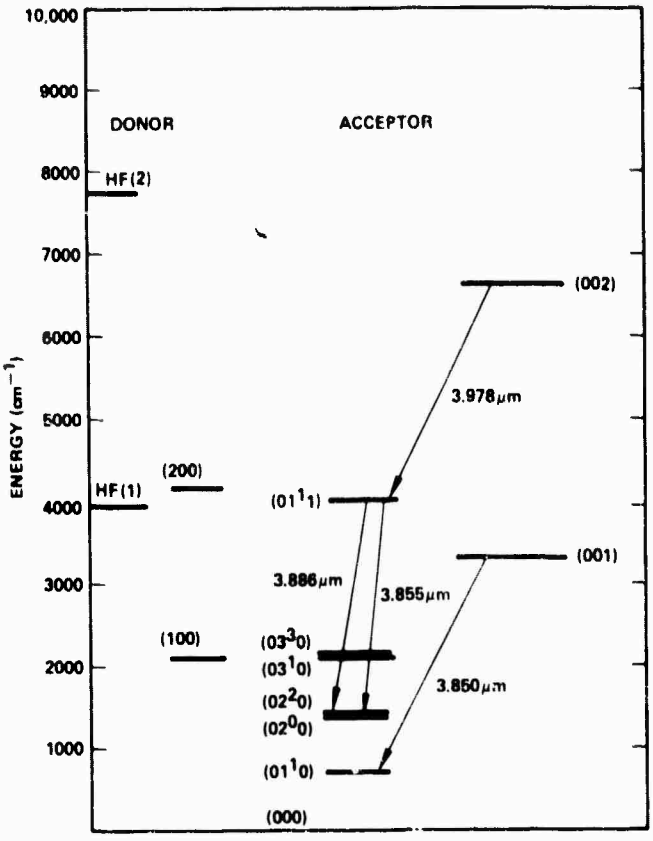

Figure 32. HF/HCN energy level diagram

TABLE 4. LASING DEMONSTRATION EXPERIMENTS SUMMARY

Maximum Value	System		
	HF	HF/DF	HF/HCN
Output (watt)	20	25×10^{-3}	Closed Cavity
Gain (cm^{-1})	≥0.03	$\geq 1.7 \times 10^{-3}$	$8.3 \times 10^{-4} - 1.7 \times 10^{-3}$
η_{CONV}	0.345	4×10^{-4}	
P_{ORTL} (torr)	110	41	41

However, its performance was far behind the single component optically pumped HF system. The relative performance can be understood on the basis of a simplified kinetic picture. As shown in Figure 33, the population density for the v = 1 level of the acceptor is dictated by the intermolecular transfer process and by the acceptor v-v exchange process. At quasi-equilibrium, $\bar{C}_o$ of the acceptor can be approximated as

$$\bar{C}_o \simeq C_o \frac{\alpha_1 t_1}{\alpha_2 k_{vv}}$$

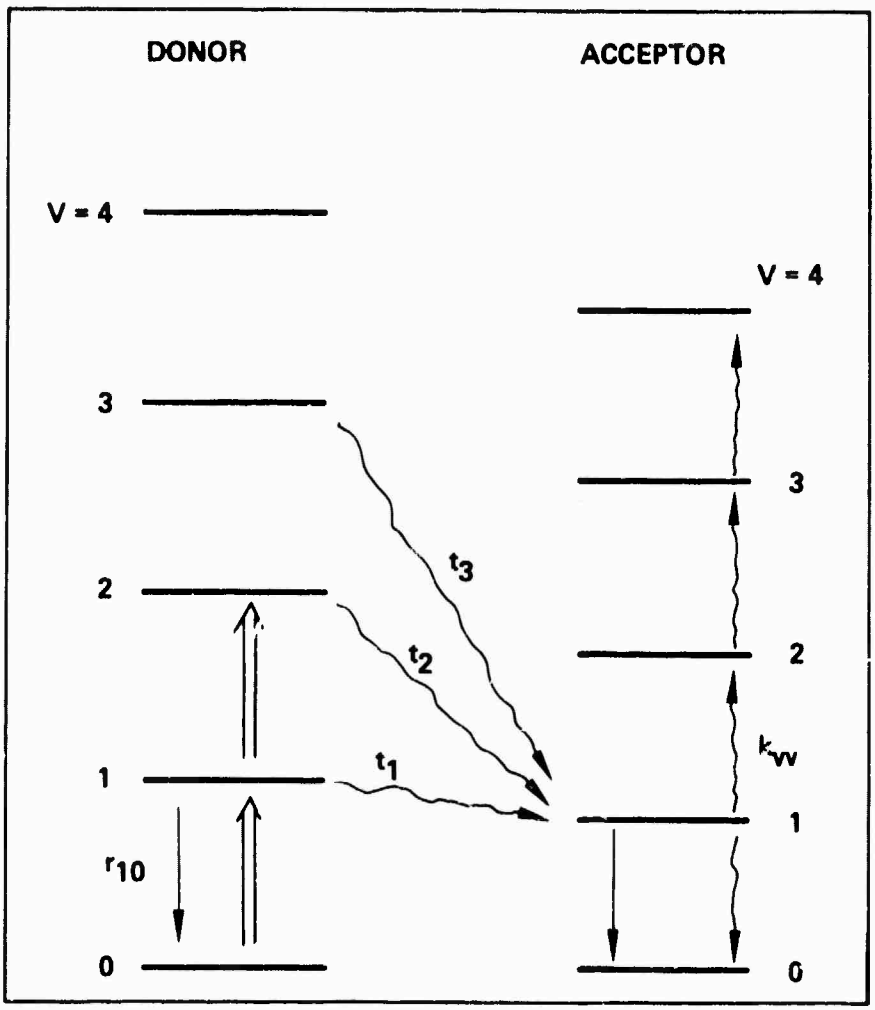

Figure 33. Two-level ORTL kinetics

where t_1 is the transfer rate coefficient for the HF (v=1) + Acceptor (v=0) → HF (v=0) + Acceptor (v=1) process and k_{vv} is the V-V exchange process rate coefficient for the Acceptor (v=1) + Acceptor (v=1) ⇌ Acceptor (v=0) + Acceptor (v=2) process, and α_1 and α_2 are the donor and acceptor concentrations respectively.

Assuming that an upper bound value of $C_o = 0.5$ can be maintained by the optical pumping process, then partial inversion in the acceptor between v=1 and v=0 (let $\overline{C}_o = 0.5$) requires $\alpha_1 t_1 / \alpha_2 k_{vv} \cong 1$. From Table 5 it can be seen that $t_1 < k_{vv}$ for all HF/Acceptor systems and this demands $\alpha_1 > \alpha_2$. In other words, in an intermolecular transfer system, because of the competition of the V-V exchange process with the transfer process, partial inversion can only be realized with $\alpha_1 > \alpha_2$. Further examination reveals that a transfer system with $\alpha_1 > \alpha_2$ is probably not very efficient. The efficiency of a transfer system can be described as

$$\eta \alpha \frac{\text{transfer rate}}{\text{Donor V-T quenching rate}} \simeq \frac{\alpha_2 t_1}{\alpha_1 r_{10}}$$

TABLE 5. COMPARISON OF KINETIC RATES IN DIFFERENT SYSTEMS

	HF/HF	HF/DF	HF/HCl	HF/HBr	HF/HCN
t_1	–	2.3×10^{-12}	5.3×10^{-13}	2.3×10^{-13}	5.3×10^{-12}
k_{vv}^A	1.77×10^{-11}	3.7×10^{-11}	4.4×10^{-12}	5.3×10^{-12}	5×10^{-11}
t_1/k_{vv}^A	–	0.062	0.12	0.043	0.1
t_1/r_{10}	–	1.04	0.24	0.10	2.4
r_{10}: HF–HF 2.2×10^{-12}					
Units are cm^3/molecule-sec					

where r_{10} is the self-quenching rate coefficient of HF. With the above assumptions with regard to inversion, η can be expressed as

$$\eta \alpha \left(\frac{t_1}{k_{vv}}\right) \cdot \left(\frac{t_1}{r_{10}}\right)$$

With the exception of HF/HCN, it can be seen that this quantity is only a few percent from Table 5. Since HCN is a triatomic molecule with a small rotational constant, it requires $\overline{C}_o \geq 1$ to have significant gain. Similar derivation will include that the similar quantity is less than 10 percent. For an optically pumped HF system, the situation is different. Intermolecular kinetics no longer put restrictions on the inversion conditions. As a result of the Screening Task, the optically pumped HF laser was chosen for detailed investigation in the remainder of the program.

3.0 PROGRAM PLANS

3.1 CHARACTERIZATION EXPERIMENTS

The remainder of the program will concentrate on the optically pumped HF laser system. A thorough experimental characterization of the behavior of this system and of the parametric dependences of system performance will be made. In addition, the range of validity of the present computer model will be assessed to the extent possible with the available laboratory apparatus. This effort will be the subject of the next technical report.

Experience gained in the first half of the program and analysis of the results have indicated the desirability of additional diagnostic capability. Consequently, several new diagnostics are being incorporated into the experimental effort. In the Screening Task the absorbed power was inferred from measurement of the laser radiation produced and from the gas temperature rise as measured by downstream thermocouples. The thermocouple measurements suffer from two limitations on precision. The first is that the temperature measurement uncertainty becomes potentially large at low pressures, because of inadequate thermal transfer. (The measurements made at 78 Torr and above, however, are of sufficient accuracy.) The second is that in travelling downstream the laser medium dissipates some heat to the surrounding helium gas curtain. As a consequence of these experimental uncertainties, it is desirable to have a direct measure of the optical absorption. This diagnostic will be added to the experimental measurements in the Characterization Task. In addition to serving as a confirmation of the measured efficiency, this measurement will at times be made using spectrometers to yield absorption coefficients for individual vibration-rotational transitions. This will allow meaningful comparisons with model predictions.

One issue that has not been experimentally addressed is the dependence of the HF excitation level on position along the flow direction. This is equivalent to the interaction time of a given molecule in the pumping radiation field. The computer model is capable of predicting the spatial profile along this axis. In order to assess the validity of these calculations,

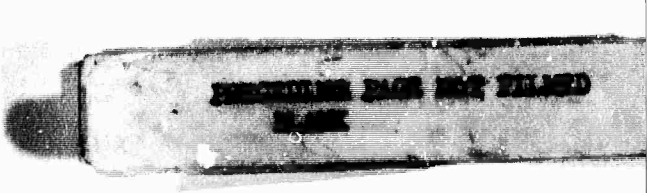

high spatial resolution scanning fluorescence radiometer measurements will be incorporated into the Characterization Experiments.

Gain measurements will also be made to yield a direct measurement of the population inversion between various states. This direct measurement will have higher precision than the fluorescence spectroscopy which measures the population in each level separately. The intracavity Fresnel loss-plate technique* is capable of measuring the loaded gain and saturation characteristics of the laser. By varying the overall cavity losses, the threshold gain can be varied and available small signal gain determined.

In addition to diagnostic improvements, other apparatus modifications will be implemented. Line selected resonators using a Littrow mounted diffraction grating will be used. Analysis of the Screening Task data also indicates that pump radiation absorption and consequently overall efficiency can be increased by using an optically thicker ORTL cell. A new wider cell will therefore be fabricated.

3.2 SCALING ANALYSIS

In preparation for the remainder of the program, the computational capability of Hughes' ORTL model has been improved. The spectral distribution of the pumping radiation after transit through the absorbing ORTL medium is now displayed, and can be compared with experimental measurements. This will also allow more optimum device design in the Scaling Analysis Task because the degree of saturation of individual pumping transitions will be able to be investigated easily. In addition, the model now allows multi-vibrational band lasing, as well as single band laser oscillation. These improvements will enhance the design capability to be applied in the Scaling Analysis Task. During this task, several device configurations will be identified and their relative effectiveness and scalability assessed. One or more of these configurations will be chosen for further analysis. Taking into account the configurations chosen, and additional experimental information, the applicability of the model will be reassessed and those additional

*J. Tulip and H. Seguin, Can. J. Phys. 48, 1086 (1970).

code modifications which are desirable and feasible will be made. Following this effort the actual device scaling analysis will be performed. Systems of interest to DARPA will be scaled and potential performance will be characterized.